FLOW ANALYSIS AROUND SERIES GROYNES OF DIFFERENT LAYOUT USING ANSYS FLUENT

A dissertation submitted in partial fulfilment of the requirement for the award of degree of

MASTER OF TECHNOLOGY

IN

HYDRAULICS AND WATER RESOURCES ENGINEERING

BY

ABHAY MASIWAL

(ROLL NO. 2K15/HFE/01)

Under the guidance of

Dr RAKESH KUMAR

Professor
Department of Civil Engineering
Delhi Technological University
Delhi

DELHI TECHNOLOGICAL UNIVERSITY
(FORMERLY DELHI COLLEGE OF ENGINEERING)
DELHI-110042
JUNE-2017

CANDIDATES'S DECLARATION

I do hereby certify that the work presented is the report entitled **"Flow Analysis around Series Groynes of Different Layout using ANSYS Fluent"** in the partial fulfilment of the requirements for the award of the degree of "Master of Technology" in Hydraulics & Water Resources Engineering submitted in the Department of Civil Engineering Department, Delhi Technological University, is an authentic record of my own work carried out from January 2017 to June 2017 under supervision of Dr. Rakesh Kumar (Professor), Department of Civil Engineering.

I have not submitted the matter embodied in the report for the award of other degree or diploma.

Date: Abhay Masiwal

                                                                                              (2K15/HFE/01)

Certificate

This is to certify that above statement made by the candidate is correct to best of my knowledge.

Dr. Rakesh Kumar

(Professor)

Department of Civil Engineering

Delhi Technological University

ACKNOWLEDGEMENT

I take this opportunity to express my profound gratitude and deep regards to Dr. Rakesh Kumar (Professor, Civil Engineering Department, DTU) for his exemplary guidance, monitoring and constant encouragement throughout the course for this project work. The blessing, help and guidance given by him from time to time shall carry me a long way in life on which I am going to embark.

I would also like to thank Dr. Nirendra Dev (Head of Department, Civil Engineering Department, DTU) for extending his support and Guidance.

Professors and faculties of the Department of Civil Engineering, DTU, have always extended their full co-operation and help. They have been kind enough to give their opinions on the project matter; I am deeply obliged to them. They have been a source of encouragement and have continuously been supporting me with their knowledge base, during study. Several of well-wishers extended their help to me directly or indirectly and we grateful to all of them without whom it would have been impossible for me to carry on my work.

ABSTRACT

Groynes are hydraulic structure constructed across the river either to control the flow of the river or to deviate the flow away from the protected bank. These can be of various types based on the material used for the construction or depending upon the shape of the groynes constructed. Generally, we do not try to construct the single groyne in the flow field as it has more ill effects than its advantage. So study of flow around the series groyne become important. In series groyne analysis, study of flow around all groyne will a difficult task specially if done by lab experimental models. In this study flow pattern around series groynes of different layout has been analysed using ANSYS Fluent. Four model of groyne are formed based on Uijttewaal experimental model. Groyne models are different from each other's on the basis of their intrusion length, tip slope or permeability. Plots of velocity, shear, TKE is plotted on different section of the flow channel. Tip velocity near the fourth groyne is compared with experimental results. Plot showing horizontal velocity profile and vertical velocity profile are useful for getting the idea that which groyne might causes maximum shear and will have vortex formation near the tip. Plot of streamlines, velocity vector and contours of shear and TKE is useful for visualizing the flow. Amplification factor of different parameters are studied for knowing the intensity of disturbance caused by groyne shape. For best layout of the groyne location and magnitude of parameters are compared.

TABLE OF CONTENTS

LIST OF FIGURES

LIST OF TABLES

Chapter 1 INTRODUCTION

1.1 Introduction

Groynes, also renowned as Spurs, are hydraulic structures generally used for river training works. Groynes extends from the bank of the river in perpendicular direction or in the direction which is at some angle to the watercourse. They could be constructed by using gravel, stone, earth, rock, or piles, beginning at the river bank with a root and ending at the regulation line with a head.

Few of the major functions performed by groynes are:-

   i.   They tends to keep the mainstream flow at the centre so that the velocity near the banks is reduced, by this bank can be protected;

   ii.   As they contract the width of channel available for flow causing an increase in the depth in the river, which is more desirable for navigation;

   iii.   As low-velocity zone are formed near river bank so sediment gets deposited and this helps in alignment of channel;

   iv.   Restoration of fish habitats and river ecosystem
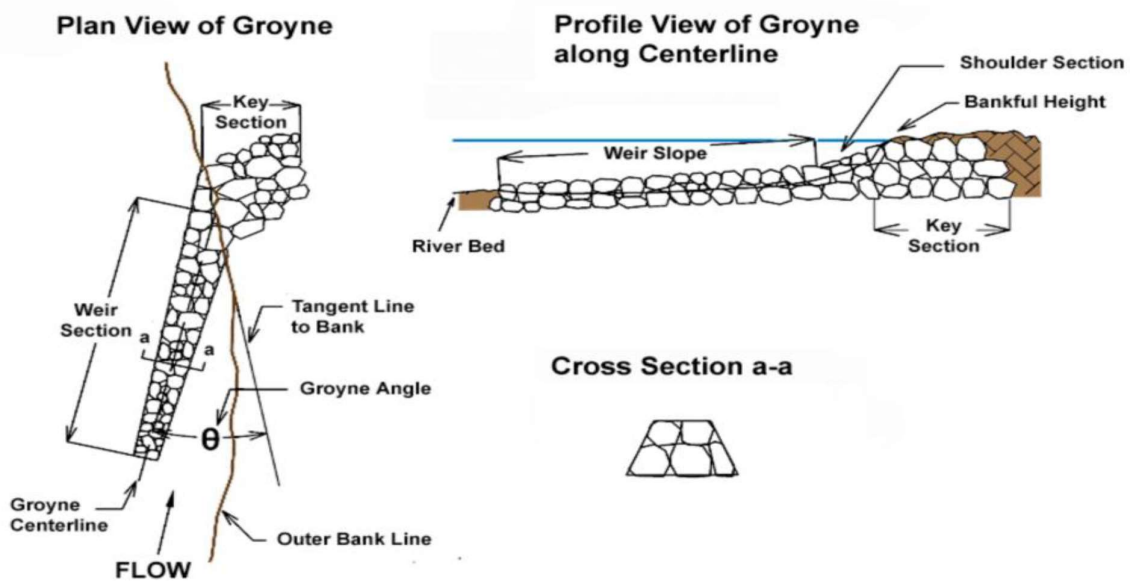
Figure 1.1 Plan, Profile & Cross-Section Views of Groynes Used For Bank Protection

1.2 Objective of Dissertation

The objective of this dissertation is:

i. To obtain the flow pattern near the series groynes of different layout.

ii. To obtain variation of velocity variation in respect of protected bank due to different models of groynes.

iii. To obtains variation of shear stress variation in respect of protected bank due to different models of groynes.

iv. To identify the maximum values of different parameters in the area near the groyne 4 and its position from the tip of groyne.

v. To understand the velocity variation in vertical and horizontal plane.

vi. To find out the value TKE induced due to placement of groynes.

vii. To find out the most appropriate model out of the four model formed.

1.3 Scope of the project

The present study focuses on studying the effect of groynes of different layout over the flow field. The study of tip velocity can be used to study scour factor near groyne. The variation of velocity and shear stress over the flow field can be helpful in understanding the behaviour of different groynes in the series as well as comparing layout effect of different model. Location of maximum shear can be useful for identifying the nearby area of potential scouring. The analysis of the shear stress field at the bed of the channel presents a particular interest for studying the sediment transport around a spur dike. The study of TKE and location of maximum TKE tell us about the area where formation of eddies is high and disturbance is also more. The result of the present study will tell us about the better groyne model layout out of various constructed and how change in the layout affects the flow field. ANSYS Fluent has been used throughout the project to analyse the flow around the spur and tip velocities, maximum velocities, maximum bed shear stress and maximum TKE has been calculated. This software contains many models for turbulent flow analysis but here the simplest model has been used to analyse the flow to understand the work easily.

1.4 Types of Groynes

Groynes can be classified on the basis of:

i. **Material and method of construction**: Permeable or impermeable. Permeable groynes allow water to pass through their body and are generally used in channels which has higher quantity of sediment load where we desired that sediment gets deposited around the groynes. There are also useful in case of milder bends or rivers having low flow rates. They can be constructed using timber, bamboo or piles. Whereas in case of impermeable groynes they don't allow water to penetrate through their body, hence deflect the water currents from their original path. They are useful in case of bank protection, provides higher depth of flow in centre of the river, which is crucial for navigation purpose. They can be constructed using rocks or gabions.

ii. **Submergence**: Submerged or emerged.
This classification depends upon the depth of water. Most of the time we impermeable groynes are designed as emerged this is due the reason because impermeable groynes experience high scour near their own body if they are constructed as submerged. Permeable groynes can be designed as submerged because of less scours near their body.

iii. **Action of stream flow**: - straight, attracting and repelling.
Inclination of attracting groynes is towards downstream, therefore they attracts the flow towards themselves causing formation of scour hole near to the bank. So these are considered as less effective for the purpose of bank protection. Intrusion of straight groynes are in direction perpendicular to the bank line and they merely changes the flow path river. Inclination of the repelling groynes is towards upstream direction due to this they repel the water mass away from the protected bank. These are generally considered as most appropriate for bank safety.

iv. **Appearance in plan view**: This comprises 'T-head', 'L-head', 'hockey', 'inverted hockey'.
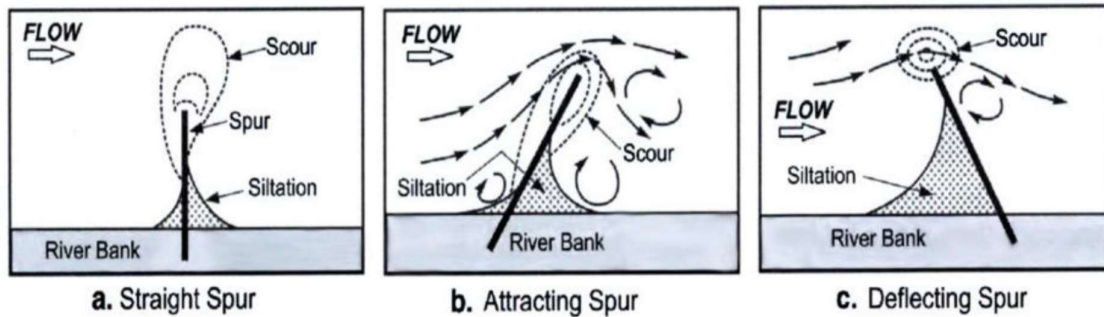
Figure 1.2 Classification of Groynes by Action on Stream Flow
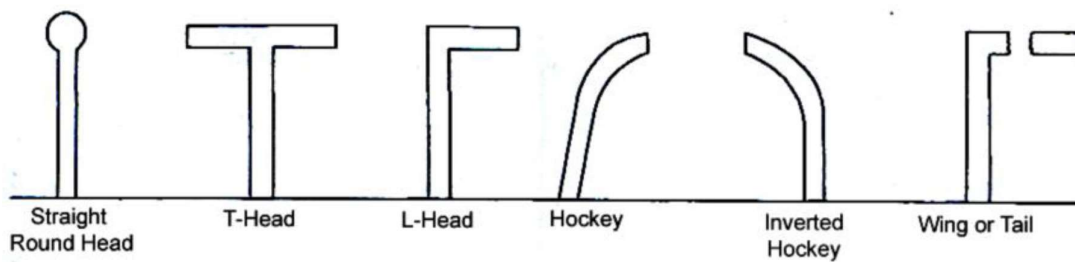
Figure 1.3 Classification of groynes by appearance in plan view

1.4 Design considerations for Groynes

The vital considerations for design of groynes are:-

a) Length of Spurs: Its length will be governed by the location, purpose, spacing, and financial side of construction. The length can be determined by defining the channel width and depth anticipated.

b) Spacing of Spurs: The spacing in the middle of Spurs is calculated by measuring the distance of the river bank between their first points. It is interrelated to river width, spur length, velocity of flow, angle to the bank, alignment to the flow, bank curvature, and purpose.

c) Plan view form

d) Orientation of Spurs: Spurs can be sloping perpendicular to the bank or be tending either upstream or downstream. Every orientation upsets the stream in a dissimilar way and outcomes in diverse settlement of sediment in the locality of the spur.

e) Cross-section of Spurs

f) Crest height and gradient

g) Construction materials

h) Scour: The predictable scour depth must be taken into design calculation in the purpose of finding the base depth of the Spurs.

1.5 Flow near Spurs
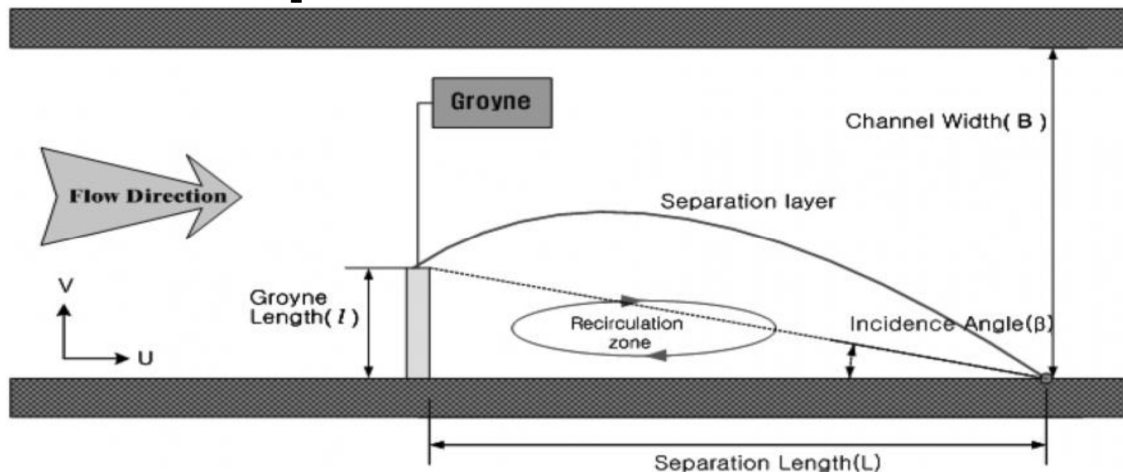
Figure 1.4 Recirculation zone in downstream of spur

For understanding the flow near groynes we generally draw the flow pattern shown in fig 1.4, this fig shows the pattern attains by water mass in the vicinity of groyne after the its installation. In the zone in-between the tip of groyne and the opposite bank the flow velocity increases, because the width available gets contracted. This zone is termed as the main flow zone. The return flow zone or recirculation zone is found at the downstream side of the spur. Variation in the velocity exists among the mainstream zone and the recirculation zone, due to which there is a development of a shear layer among the dualistic zones. A large vortex take place in the recirculation zone and in the vicinity of this large vortex there are formation two small vortex. As we move towards the downstream there is mixing of these two zones and consequent the recirculating zones mixes with the mainstream flow. Distance between the initial point of the groyne and the point where mainstream again touches the protected bank is termed as separation length.

1.6 Introduction to ANSYS Fluent

Computational Fluid Dynamics (CFD) is a tool used to analyse condition, it uses set of mathematical equation to be solved in computer for obtaining the results. In the numerous engineering field, we can found a drift that there is an emerged attentiveness towards the CFD analysis. The basic idea behind using CFD is to analyse the fluid flow in detail and this done by converting the continuous flow equation for the region of interest into the discretised mathematical sets of equation, by applying various boundary condition which are know in advance. Growing use of CFD as analysis tool is due to its advantage of precise modelling, accurate results and less computational cost.

One of the CFD solver used for analysing complex flow is ANSYS Fluent. ANSYS Fluent is incorporated within the ANSYS Workbench platform. ANSYS Fluent provide the option for geometry construction and meshing. It can also solve the unstructured mesh, which is useful to mesh around complex geometries. ANSYS Fluent supports various mesh type like quadrilateral, triangular, tetrahedral, hexahedral and polyhedral. Commands like proximity and curvature helps in smoothing the mesh near the various curve and sudden cut sections. The software also provide the option of dynamic coarsening or refinement of the mesh size, which ultimately helps in obtaining the accurate results or on reducing the run time required for analysis. ANSYS Fluent can be used for all types of models and flow like transient or steady-state flow, incompressible and compressible flow, turbulent and laminar flow. ANSYS Fluent provide the option to the user to adapt from various type of models that is applicable for the given conditions. In the real life situation, most of the open channel flows are turbulent in the nature so ANSYS Fluent more turbulent models like one equation model or various two equation model. ANSYS Fluent also provides tools which enables the user to choose the material either it of fluid flowing or the material from which channel is constructed, this allows more realistic conditions. Number of iteration can be varied according to the experience that in how many iteration model will get converged. ANSYS Fluent has its own embedded Post-processing tools which enables the user to obtain various contours, velocity vectors, streamlines,

animations, graphics and various other sets of representative results that useful for analysis of fluid flow.

With all these tools within a single software, it became easier for the user to create a model then solve in and in the same software analyse the results found.
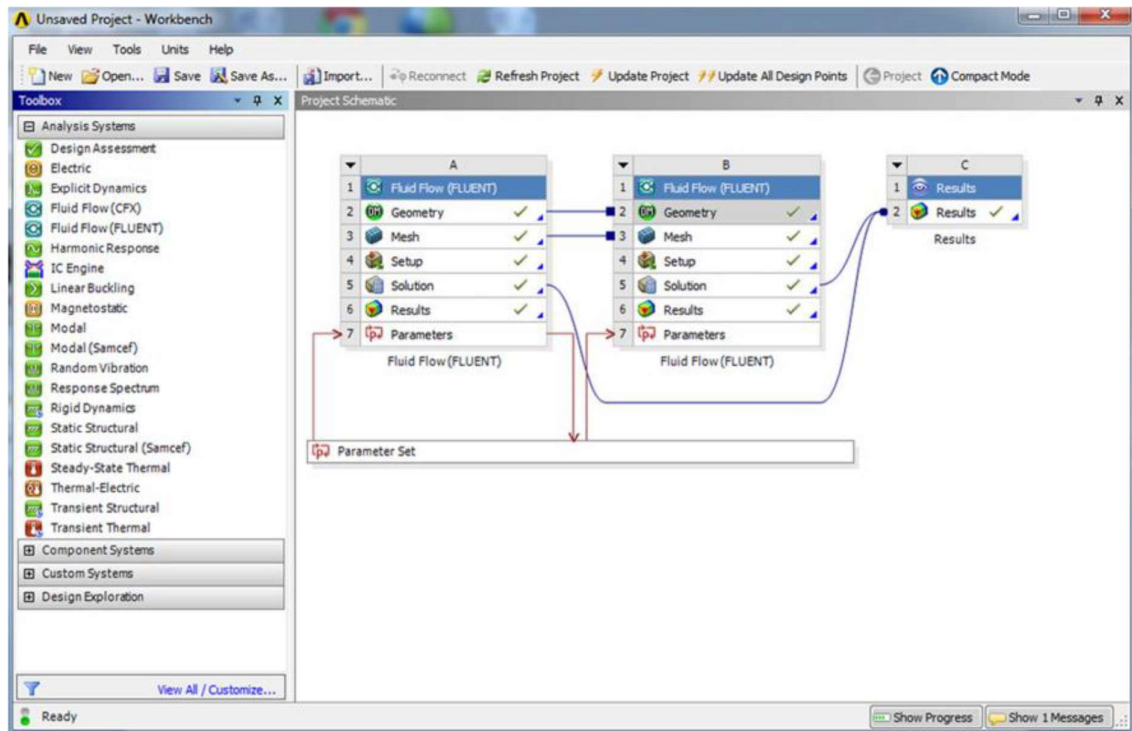
Figure 1.5 Overview of ANSYS Fluent

Chapter 2 LITERATURE REVIEW

In this dissertation work, various research papers are referred which are enlisted in references. Many researcher performs experiment for the purpose of study of flow near the groyne or to study the effect of groyne size on the flow patterns. Some the research done is described in this chapter.

Uijttewaal *et al.* [20] provided detailed information about the flow pattern, turbulence properties and development of shear layer around a particular groyne head by conducted different experiments at a groyne head. It can be concluded from the results that the turbulence properties can be greatly influenced by the design of groyne at the interface of river and groyne. The groyne would not only change the structure of the riverbed but also the resistance of the flow in the river and transportation of matter from one place to another. The study will be helpful in optimisation models of the river system in different aspect of navigation and flood prevention works. The different aspects of the groyne have been still examined in different aspects for the judgment of practical importance of the groyne type. In this model, the conventional Type A had been totally improved by adjusting the permeability, shape and the groyne tip in place of reduction of the horizontal velocity gradient around the groyne field. The results show that the flow field had been changed completely by the variation of water stages at different points in the river.

Jirka *et al.* [22] conducted his experimental research work on the study of the effect of dead zones i.e. groyne fields and harbours on the river in the longitudinal direction. The objective of the study was the development of the improved model of travel time by injecting tracer cloud at maximum skewness and concentration as compared to existing models. The longitudinal stretching of a tracer cloud in downward direction of river have greatly influenced by the exchange processes between dead zones and mainstream. At the head of a groyne, the two-dimensional and coherent structures had been developed which was responsible for the exchange process between the

mainstream and the dead zone. Because of the shallow flow in the river, the growing structures were developed in the horizontal direction.

Zhang *et al* [27] presented an experimental study on the bed variation characteristics and the corresponding flow structure around different types of groynes in sediment mixtures. Impermeable and permeable spur dykes were combined in various ways and their hydro-morphological implications were investigated.

Minor *et al* [12] found that the results of three-dimensional numerical modelling had provided detailed inspection about the predicted three-dimensional velocity field in the range of barbs. From the detailed analysis, it can be concluded that in a barb field the stream traces generation and the calculation of vorticity gave comprehensive view of the characteristics of three-dimensional study. The characteristics of the flow field in the river could directly affect the magnitude and pattern of erosion and sediment deposition in a channel. This pattern would be changed in a channel bend by the addition of barbs or other flow in the stream structures. For the protection of bank of stream and deign the barb in optimise way the detailed understanding of the flow pattern is required.

Sarkardeh *et al* [24] et al done analysis over a single groyne with free surface, they conducted both laboratory experiment as well as analysis of mathematical model using Fluent. In their model, they used Navier-Strokes equation to perform analysis of three-dimensional flow. To study the effects of turbulence relating phenomenon they used k-Є model. For understanding the effect of groyne over the free surface they used volume of fluid method in which two-phase are taken as air and fluid phase. Meshing of the model is done by both structured and unstructured mesh, density of mesh was higher near to the groyne wall and free surface to obtain more accurate results. In their model, they performed analysis over repelling, attracting and straight groynes of different lengths. Velocity contours over the flow field, shear stress

on the bed of the channel, streamlines were drawn to study the effect of the groyne.

Robert *et al.* [7] conducted various experiments on several flume on small scale model to study scale effect over the flow around a groyne placed on a bed whose bed is flat. The prime interest of these experiments are to find the line of maximum velocity and found the separation length which determine the wake region downstream the groyne. Use of small-scale model is to study various parameters which are primarily affecting the channel control issues. In these experiment researcher used shear stress on the bed and Froude number as parameter for the studies, general shear stress is used as criteria where there is loose bed material which is susceptible to scouring and Froude number is used as criteria in cases where the gravity forces as predominant over the other forces as in case of open channels.

Ahmed *et al.* [2] to study the effect of impermeable groynes on the flow field carried out an experiment in which they prepared a wooden symmetrical compound channel. Different relative length of the groynes are placed in both single groyne pattern as well as in series pattern. In this experiment, an impermeable groyne had been used with a large relative length which generated flow eddies on a river flood plain and creates separation zones in the downstream of the groyne as well as in the upper region of the main channel. As a result of this process, the floodplain erosion had occurred. From the observations, it was found that in the upper region of the main channel the velocity had decreased but in the lower and middle region, the velocity had increased. The increment in the velocity was also occurred in the other floodplain. The negative velocities reached at –20%, –30%, and –55% of the original velocity when the single groyne length was considered as $Lr = 0.5$, 0.75, and 1.0, respectively. These negative velocities were replaced by the increment of the flow velocity in the main channel of the river as well as on the opposite flood plain. As a result of this substitution the increase could reached at the level of 1.4, 1.6, and 1.85 times of the original velocity in the main channel and 1.75, 2.25, 2.75 times of the original value on the flood

plain. On one side of the flood plain, it was found that the effective distance between the two symmetrical groynes varies from 3 to 4 times the original groyne length. Due to the weak protection works for reducing the effect of scouring process the embankment failure and river levee can occur. As a result, the centre line and flow of river can change easily. These effects can be reduced by maintain the length of groyne less than half of the floodplain width. They measured the water depth near the groyne and velocity of flow primarily to found out the influence of groyne length. They also tried to set up an adequate range for the spacing between the groynes in series pattern. In their results, they found that the increased in velocity near the groyne is of the order of 50%, 85%. They also found out that more relative length of groyne cause eddies formation in downstream to the spur. So for relative length, they concluded that relative length should be less than half of the total width. Range which they suggested for spacing between the groyne lies in between 3 to 5 times the length of the groyne.

Schmidt *et al.* [15] carried out experiment to find study recirculation flow and the volume of sedimentation in lateral eddies during the expansion of the channel. They conducted 30 hours experiment during which they added mixed sediment particle to the main flow. The conclusion regarding their experiments are that reattachment point can be considered as point where the expanding vortex again touches the wall, and this point generally in the range of 5 time the height of step. They also found out that I some portion of recirculation zone the instantaneous component of the velocity changes its value over the entire range of 360-degree.

Tambe et al [18] done their experiment on 10 m long, 0.30 m wide rectangular channel to find out appropriate spacing between the permeable groynes. They used acrylic model of different permeability like 30%, 40%. They found out that spacing between the groynes depends upon the width of channel, velocity of main flow, depth of waterway required and characteristics of bed material. They concluded that spacing between the groyne is very crucial parameter that affects the stability of groynes and also their ability to protect the bank.

Yeo *et al.* [24] performed the experimental study to evaluate the influence factor of different interval of groynes. They measured the flow pattern near the groynes and measured the variation of recirculation zone with respect to approach velocity, variation of permeability, installed angle and groyne length. They also measure the groyne tip velocity of the permeable and impermeable type of groyne and scour factor at near the groyne. The LSPIV technique was used to measurement of recirculation zone. For the measurement of tip velocity, the velocity difference ratio was observed on the basis of permeability. In the impermeable type, the measurement was done by increasing the value from 1.25 times to 1.7 times and for the permeable type, the smallest had been taken as 1.1 times. The slight deviation was observed in most of the incidence angles with increasing the groyne length. The value of these was taken as 5º, 6º, 10º and 20º for impermeable, 20% permeable, 40% permeable and 60% permeable groyne, respectively. It was observed that with the increment of groyne length the incident angle was decreased from 45º to 30º at 80% permeable groynes. The results of the experiments were given as an empirical equation of groyne length and tip velocity with the permeability.

Dartus *et al* [13] presented the porosity method for computation of flow for free surface and its application was used with 3D Reynolds solver by using the application of SIMPLE algorithm. The test was performed in a wide rectangular channel with concerns with the flow around a groyne. From the results, it was observed that the computed water depths were agreed with the experimental data. The major errors were found less than 0.5% which caused by the underestimation of 7% in the reattachment length.

Maheswaran *et al* [19] computed the average depth velocity and shear stress distributions at the bottom of the rectangular channel at near a groyne by using a Two-Dimensional Model. To solve the turbulence transport and governing equations of flow the model used the iterative method and hybrid finite difference scheme. A correction factor was introduced into the *k-e* turbulence model in the region of groyne tip to reduce the effect of curvature

effect of streamlines. As compared to the previously given numerical methods this model improves the agreement between the experimental data and computed values of the velocities. In this region, due to the 3-D effects, the bottom shear stress was greatly influenced by the bottom shear stress. For improvement of computed bottom shear stresses a Three- Dimensional correction factor was introduced. The sensitivity analysis was made on the streamline correction factor for curvature, on the *k-e* model coefficients and 3-D effects. The analysis had been done for the measurement of experimental error in measurement of bottom shear stress and the velocity. The computed average errors between the previous experimental results and computed values were presented with confidence intervals.

Nwachukwu *et al* [14] presented the experimental results of the turbulent flow near the structures of groyne. The deflected flow through the groyne had been analysed by using the three-dimensional flow through the turbulent boundary layer. In this case, it was observed that the flow was bounded by the groyne, separating streamline, the groyne and the adjacent bank shear layer in which the velocity profiles had been found to be similar. The disturbances were observed in a short distance and long distance in upstream and downstream, respectively. The analysis of the disturbed flow had been done by separated it into shear layer and deflected flow region. The turbulent boundary layer model in skewed form of Johnston was found true for deflected region.

Baba *et al.* [4] investigated the characteristics of flow around the spur dike by using experimental studies which carried out with the help of an electromagnetic velocimeter and the LSPIV technique. The longitudinal length of recirculation area and distribution of velocity were calculated. The experimental studies were performed on both some impermeable and permeable dikes. From the results, it was concluded that in terms of morphodynamics appearance around the spur dike the permeable spur dike appears shows better alternatives as compared to impermeable spur dike.

Acharya et al. [16] carried out the experimental study around the three dikes which was in series and presented a 3D numerical simulation of turbulent flow field. This problem was solved with the help of Flow-3d software. For comparison of different experimental data, they used three different numerical models. From the study of results, it was found that simulated mean flow field was very close to the experimental data.

Asayama *et al* [1] measured the bed morphology and size of groynes by conducted various field investigations. The performance of bed variation around the groynes, numerical analysis of Three- Dimensional Flow and Particle tracking velocimetry had been carried out. For stable bed morphology, a river structure was proposed in term of simple arrangement.

Duan *et al* [6] carried out the experimental study around the spur dike placed in a fixed bed open channel with the help of micro-acoustic Doppler velocimeter in three-dimensional turbulent flow fields. The evaluation of turbulence and mean characteristics had been done in upstream and downstream direction of the spur. The maximum bed shear stresses were found out three times more than the mean bed-shear stress of incoming flow by using Reynolds stresses.

Ettema *et al* [7] determined the scale effects of flow in models of small-scale around a single spur dike that placed in a flat and fixed bed channel. The different parameters such as flow - thawleg alignment and recirculation zone were studied. They showed that these parameters influenced by use of a shear stress parameter as the basic criterion for dynamic similitude. The reason of this was the distortion of pressure gradients around the dike of model and by the effect of generation of turbulence by the dike. It was also shown that for small models range, extent of separation region and thalweg alignment did not scale with the scales of model length.

Ghaidarbandi *et al.* [8] studied the effect of the groyne wall slopes and cross shore on flow parameters around an impermeable groyne by considering

three-dimensional numerical model i.e. FLUENT software. For analysis of the flow, they used k-ϵ RNG model. They concluded that by increasing the bed slope of cross-shore the magnitude of bed shear stress and maximum velocity was decreased.

Kafle [9] solved a numerical model to simulate the 2-D flow near a spur dike. To simulate the flow field around the spur dike that introduced at 90° of the flow in a fixed flatbed the CFD program (Nays 2D) was used. To achieve the best results, several turbulence closure models, constant eddy viscosity model and zero equation models were applied and compared. The simulated results of the study were compared with the existing and computed and experimental data.

Kang et al. [10] carried out the hydraulic experiments by varying the bed in fixed and movable condition to examine pattern of flow, scour depth and hole around a groyne. The testing was done in both permeable and impermeable groynes. With increasing permeability, the maximum scour depth was moved linearly in downward direction for each groyne type and the scour depth was decreasing with the increment of permeability. The maximum scour depth was found greatest for perpendicular groyne. The scour area was larger for impermeable groyne as compared to permeable groyne.

Safarzadeh et al. [15] conducted experimental study for measurements of the head shape effects on the bed shear stress distribution around T-shape groynes and a single straight groyne. Shear stress distribution was found more uniform in the downstream of the T-shape groyne.

Shahrokhi *et al* [16] provided a numerical model of groyne by using Flow-3D software. They used it in surrounding flow by using large eddy turbulence model while studying the effects of these factors on separation length and width of separation region behind a groyne by applying various installation angles, groyne lengths and flow velocities. For angle of installation of 105° the separation region length and width were found maximum.

Chapter 3 METHODOLOGY

3.1 Overview of Experiment

Experiment was conducted by Uijttewaal W.S.J[20] in laboratory of Delft University of Technology, Netherland to study the effects of various groynes shapes in the groyne field. For conducting the experiment a 30 m long and 5 m wide flume was chosen which can give sufficient space for placement of five groynes in series. Model of groyne was taken from Dutch river Waal and geometrically scaled to 1:40. Scaling is based upon the Froude number law as Reynolds number always remain higher in the turbulence range.
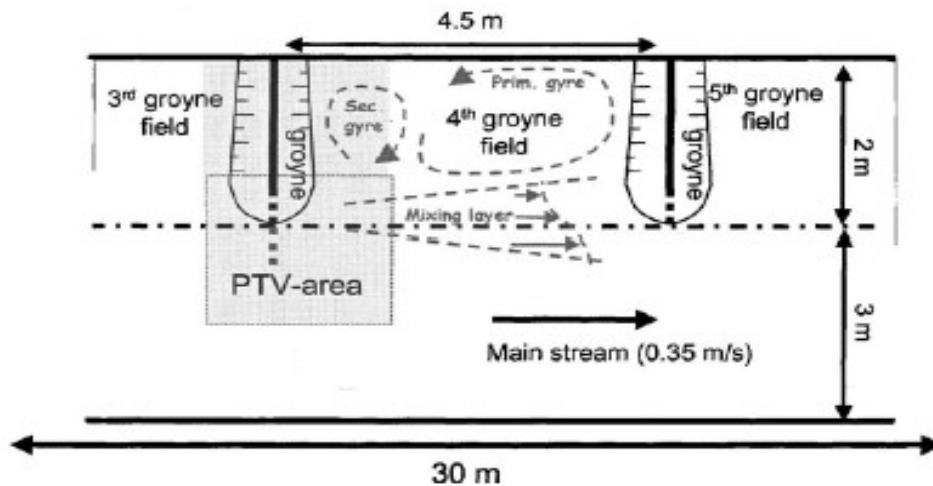
Figure 3.1 Schematic Diagram Showing Experimental Setup

Five similar groyne are placed in series with spacing of 4.5 m between them. Study area in this experiment kept as 4th groyne field as initial groyne field show some deviation from those which are downstream. Fifth groyne is placed to avoid the outlet effect.

Area blocked by all the models are kept constant so as to maintain same average velocity in all types of groynes. The height of the groyne is kept as 0.25 m and depth of water level also kept as 0.25 m. flow velocity in the main channel is 0.35 m/s with Froude number equal to 2.

Velocity Measurement: velocity is measured with the help of Particle Tracking Velocimetry (PTV). Measurement of velocity was done at various location

especially on the mixing length and area near to the groyne location. For the rectangular part of 1.5 m by 1.5 m, time series of 5 min duration were recorded. Every frame contains 2 mm diameter particle 2000 in number moving on free surface. Then velocity of these particle were calculated using an algorithm called PTV algorithm. The vertical profile of velocity and spectral distribution of turbulence kinetic energy is studied with the help of submersible two-dimensional Laser Doppler Anemometer.

3.1.1 Physical Models

In the experiment, four different model are tested. In each model, there is difference in shape of the groyne and its permeability. The first groyne model is present in the river and then other three models of groyne have variation so as to achieve better performance. In all the groyne model total area blocked by the groynes kept constant due to this length of groynes may vary according to their respective geometrical shape. All the surfaces are made up of smooth concrete and blockage is provided with the help of square metal pipes.

M1 Model: this groyne model is straight impermeable spur intruded into the river with a slope of 1:3 at its tip. Length of groyne is 2 m.
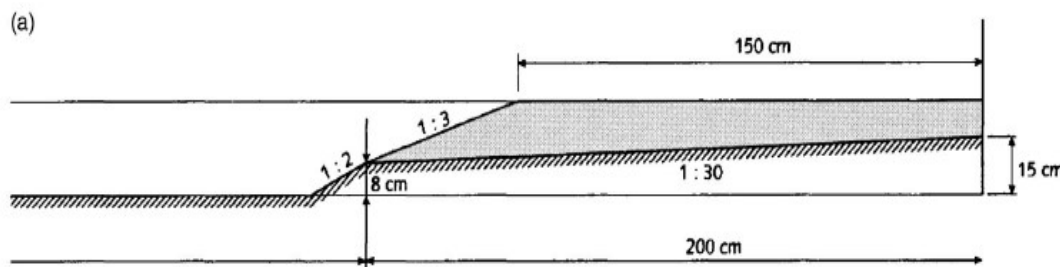
Figure 3.2 Cross-Sectional View of M1 Groyne

M2 Model: in this case, the tip slope of groyne made gentler to 1:6. As area blocked by the groynes should remain same so there will be slight increase in the intrusion length, so length of groyne become 2.5 m. This groyne model is also completely impermeable.
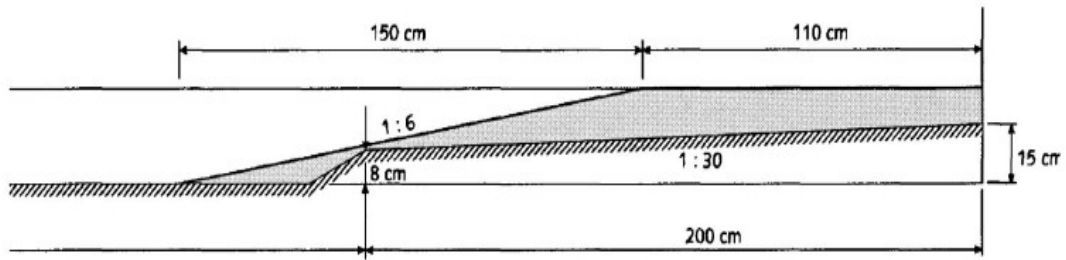
Figure 3.3 cross-sectional view of M2 groyne

M3 Model: in this case, the groyne is completely converted into permeable groyne. Permeability of groyne vary along its length. For keeping area block same the length of groyne is increased to 3 m.
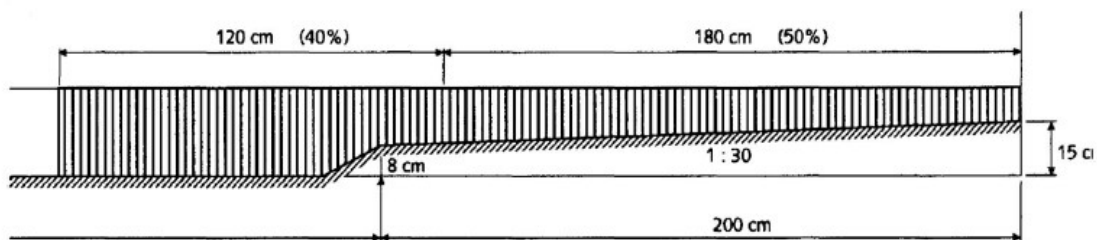
Figure 3.4 Cross-sectional view of M3 groyne

M4 Model: To include the advantages of both permeable groyne as well as impermeable groyne, in this case, groyne geometry is of hybrid nature. Length of groyne is taken as 2.5 m. bottom portion of the groyne is kept impermeable and upper part of groyne is permeable with varying permeability along its length.
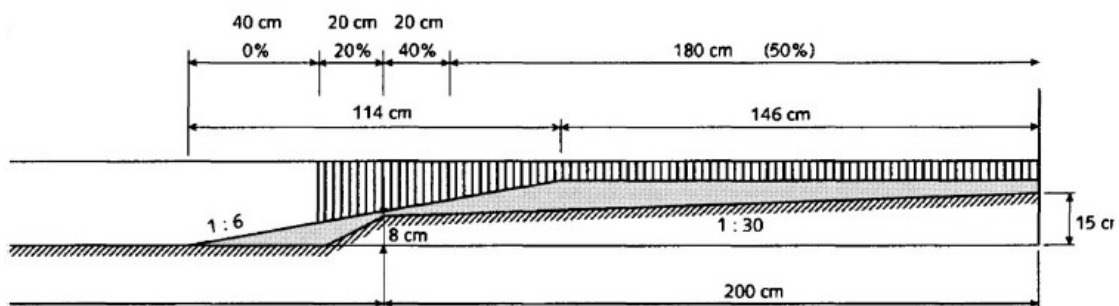
Figure 3.5 Cross-sectional view of M4 groyne

3.2 Numerical Method

For analysing these models through numerical model ANSYS Fluent is used. In numerical simulation of fluid flow undergoes following three steps:

(a) Pre-Processing
  - ➢ Construction of geometry
  - ➢ Meshing and Domain designation
  - ➢ Selecting the model to be used for solving, based on flow type
  - ➢ Providing initial condition and defining boundary condition

(b) Solver
  - ➢ To converge the solution time steps and number of iteration is selected accordingly

(c) Post processing
  - ➢ After calculation is completed various results in the form of contour and charts are analysed.

3.3 Geometry Setup

In ANSYS workbench there is design modeller in which geometry can be constructed. Total four models of groynes field is created each having series of five groynes. All the geometries are kept same as the experimental model.

Table 3.1 Model Description

Model	Length of Groyne (in m)	Symbol Used
M1	2	l_1
M2	2.5	l_2
M3	3	l_3
M4	2.5	l_4

Various dimensions used during numerical modelling of these series groynes are listed below:

Table 3.2 Dimensions of Flow Field

Entity	Value (in m)
Length of the channel	30
Width of the channel	5
Distance of G1 from starting of channel	5
Thickness of groyne	0.1
Distance between the groynes	4.5

3.3.1 Geometry of Various Model in ANSYS Fluent
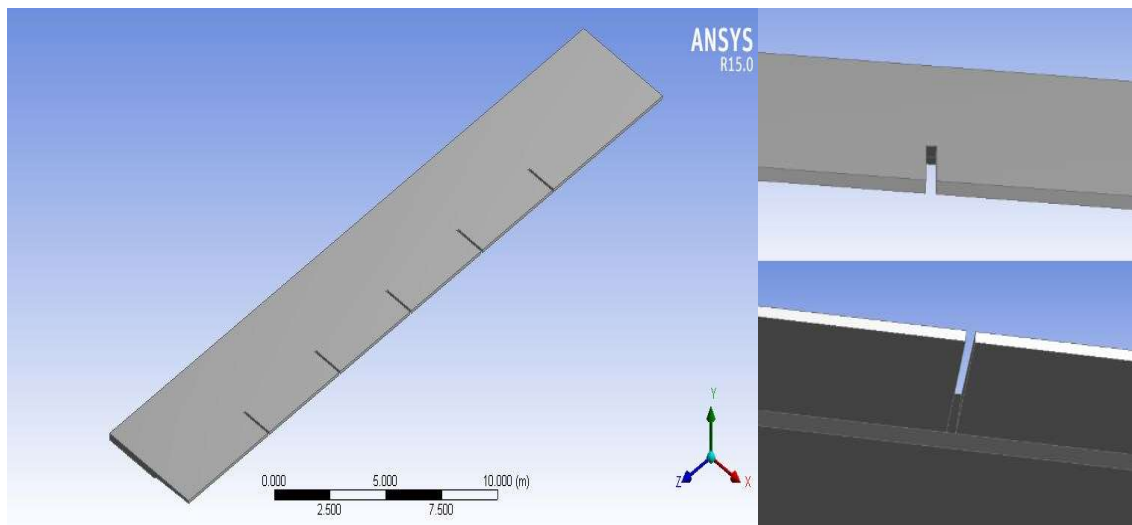
Figure 3.6 Geometry of M1 Model in ANSYS software
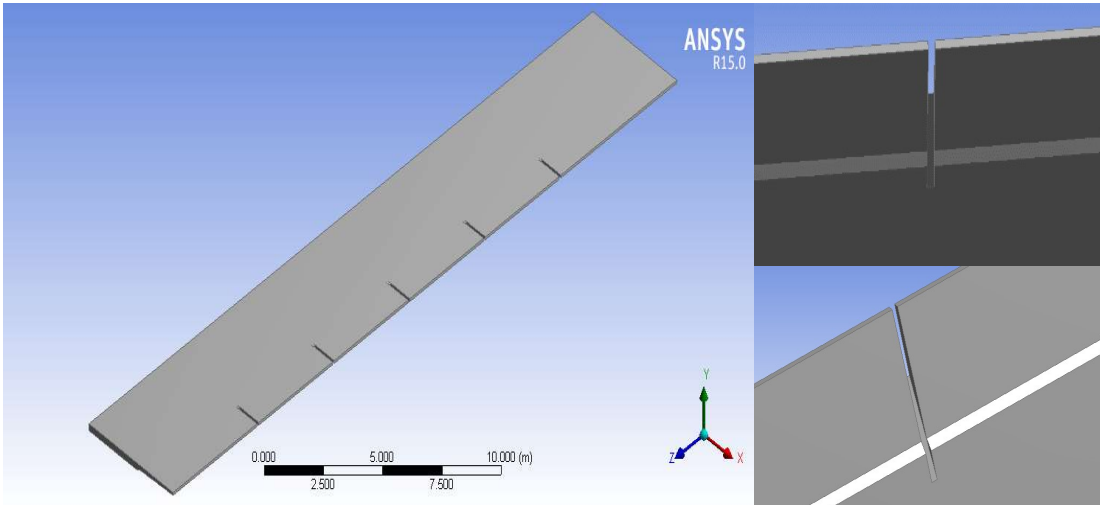
Figure 3.7 Geometry of M2 Model in ANSYS software
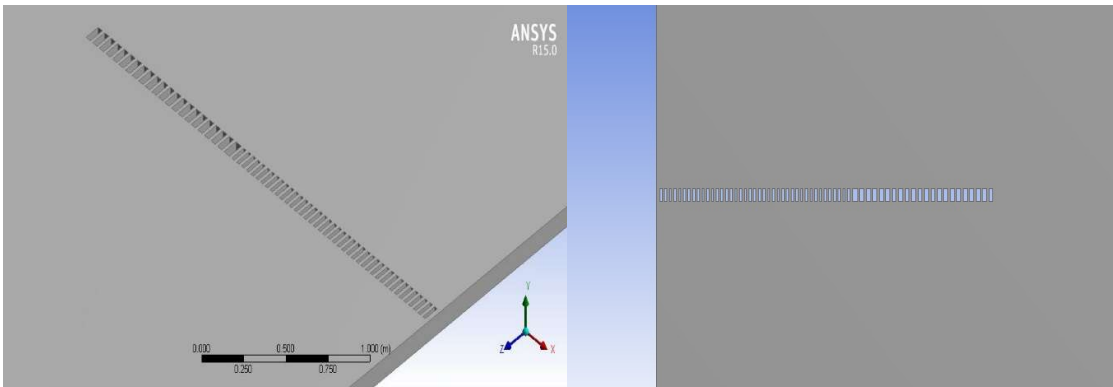
Figure 3.8 Geometry of M3 Model in ANSYS software
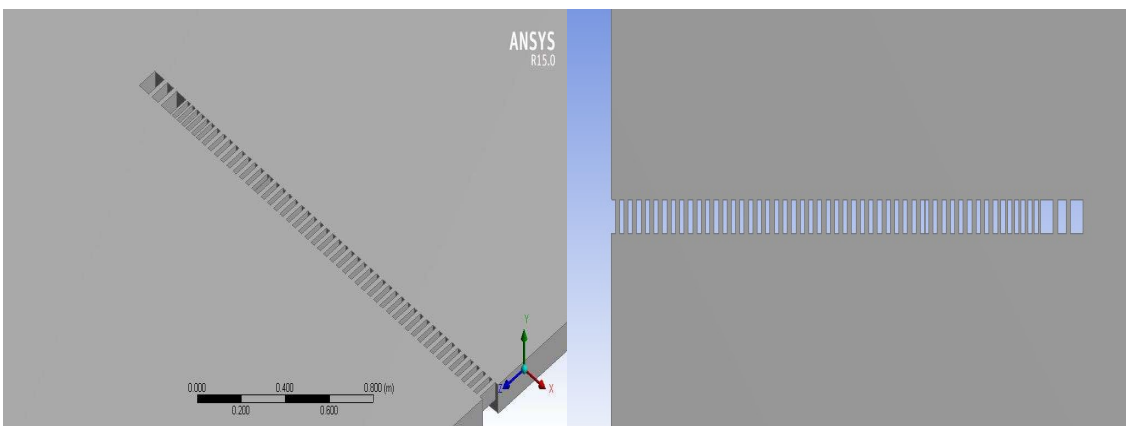
Figure 3.9 Geometry of M4 Model in ANSYS software

3.3 Meshing

Meshing tool is available in ANSYS Workbench so meshing of various model is done through it only. The desired physical preference and accuracy required will alters the mesh type and its size.
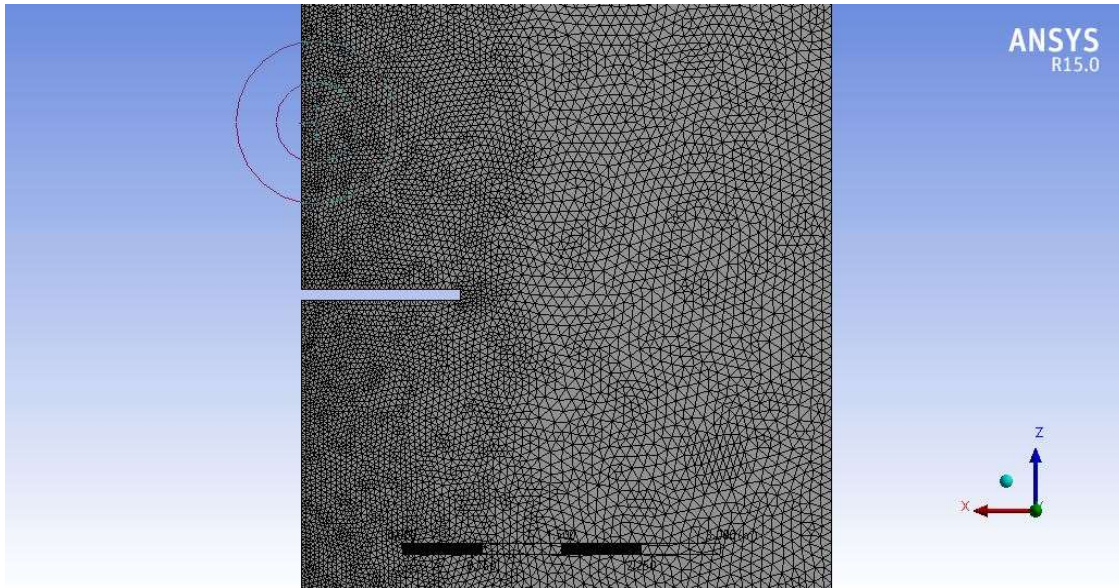
Figure 3.10 Meshing for impermeable groyne in ANSYS software
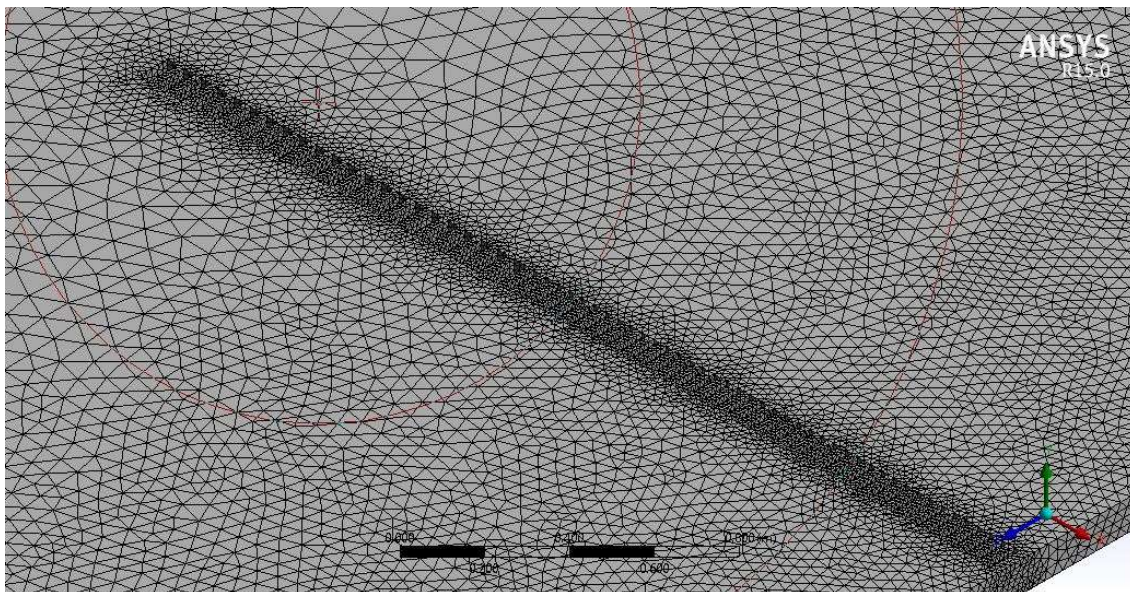
Figure 3.11 Meshing for permeable groyne in ANSYS software

In the meshing step, we also name the section which will act as different boundary parts of the model like inlet, outlet, top surface, bed etc.

Table 3.3 Mesh Description

Object Name	Mesh
Physics Preference	CFD
Solver Preference	Fluent
Used advanced function	Proximity and curvature
Mesh	Fine
Min. size	0.1 m
Max. size	0.1 m
Nodes	14951

3.4 Fluent Setup

It is the part of software where we provide the information, like input variables, boundary conditions, type of model to be used, to the software for calculation purpose.

In this, the first step is to provide details like value and direction of the gravity. Solver details like steady or transient time analysis, pressure based or density based analysis. Units of various parameter can also be changed from this interface.
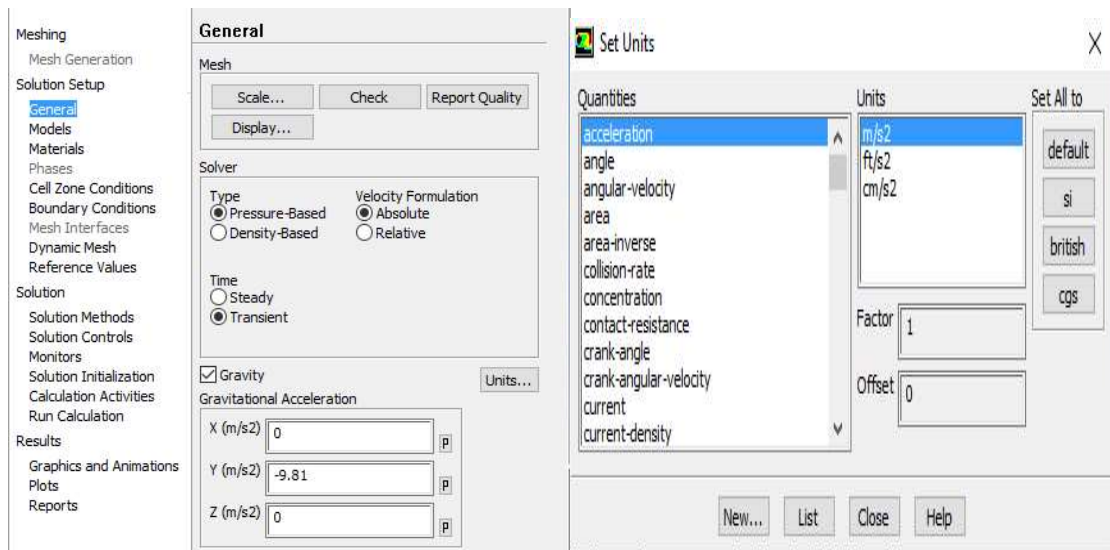
Figure 3.12 General inputs required in ANSYS software

In the next step, software provide us, numerous models, among which we select the model which is suitable to our conditions. In this case, we have selected k-epsilon model which is a two equation turbulent model. Figure given below shows name of various models that are available in Fluent for analysis.
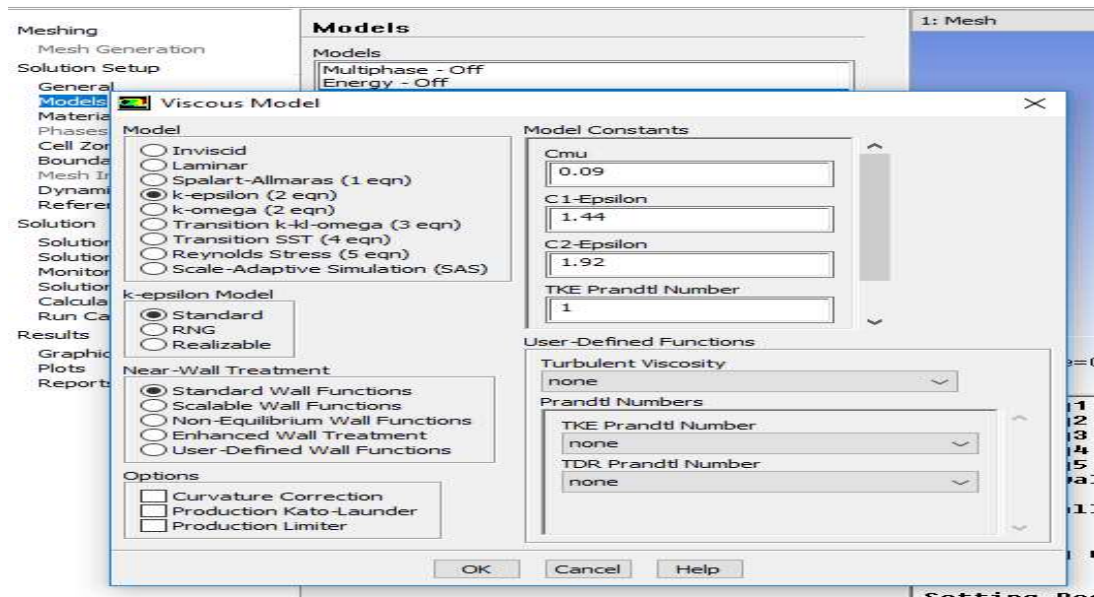
Figure 3.13 Model used for analysis in ANSYS software

Standard k-epsilon model: the basic assumption in this model is that the flow in fully turbulent and the molecular viscosity has negligible effect. It is a two equation model, in which turbulence is quantified with the help of two parameters

- o Turbulent Kinetic Energy (k)
- o Turbulent Dissipation Rate (ϵ)

The model transport equation for k is derived from the exact equation and the model transport equation for ϵ is obtained using physical reasoning. The assumption while driving k-ϵ model is that the flow is fully turbulent and the effects of molecular viscosity are negligible. The turbulence kinetic energy (k) and its dissipation rate (ϵ) are obtained from the following transport equations:

$$\frac{\partial(\rho k)}{\partial t} + \frac{\partial(\rho k u_i)}{\partial t} = \frac{\partial\left|\left(\mu + \frac{\mu_t}{\sigma_k}\right)\frac{\partial k}{\partial x_j}\right|}{\partial x_j} + G_k + G_b - \rho\varepsilon - Y_M + S_k$$

$$\frac{\partial(\rho\varepsilon)}{\partial t} + \frac{\partial(\rho\varepsilon u_i)}{\partial t} = \frac{\partial\left|(\mu + \frac{\mu_t}{\sigma_\varepsilon})\frac{\partial k}{\partial x_j}\right|}{\partial x_j} + C_{1\varepsilon}\frac{\varepsilon}{k}(G_k + C_{3\varepsilon}G_b) - C_{2\varepsilon}\rho\frac{\varepsilon^2}{k} + S_\varepsilon$$

Where,

- o G_k can be understood as the generation of turbulence kinetic energy due to the mean velocity gradients,
- o G_b can be understood the generation of turbulence kinetic energy due to buoyancy.
- o Y_m can be understood the contribution of the fluctuating dilatation in compressible turbulence to the overall dissipation rate.
- o $C_{1\epsilon}$, $C_{2\epsilon}$ and $C_{3\epsilon}$ are constants.
- o σ_k and σ_ϵ are the turbulent Prandtl numbers for k and ϵ respectively.
- o S_k and S_ϵ are user-defined source terms.

Further, we have to provide details regarding the different material which are used for the construction or are flowing. Fluent database already have properties of many material and Fluent also provide the option to users that they can create new material with known properties and can use in their analysis.
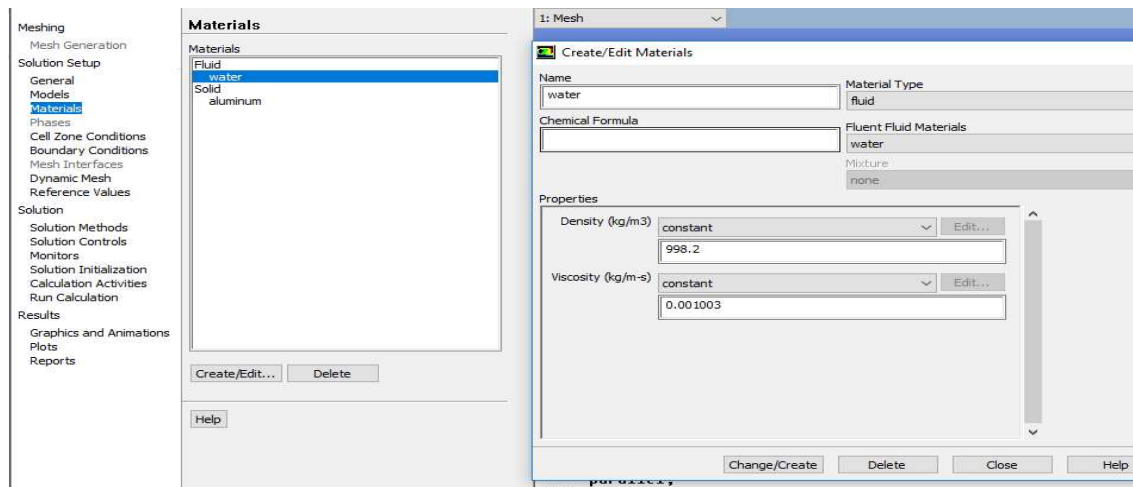
Figure 3.14 Material properties assigned in ANSYS software

In the next step, we have to provide various details regarding the boundary condition that are applied on the model like inlet velocity, outlet condition, top surface condition.

Inlet: Input flow velocity for the various models is kept constant for keeping the discharge constant. Flow velocity is so chosen that the flow in all models always remain in turbulent zone. As the layout of the various models of groynes are changing so it would be easy to study the effect of layout changes over same velocity by comparing the changes occur in the input velocity.

  o   Input velocity for all the models are equal to 0.35 m/sec.
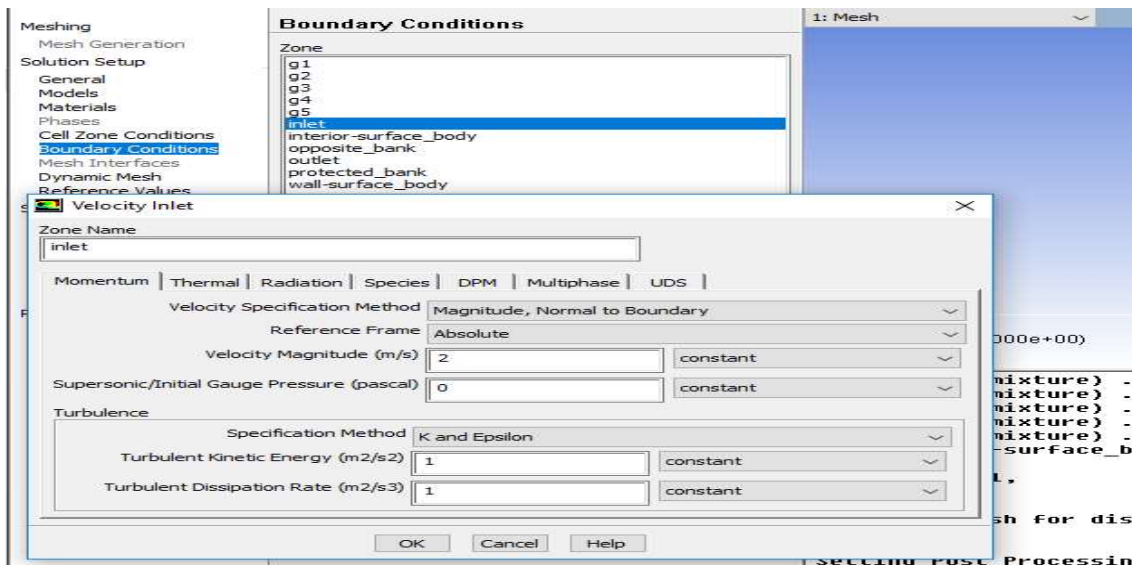
Figure 3.15 Input Velocity Provided In ANSYS Software

Outlet: outflow condition at the outlet governs the flow pattern in the flow field. Fluent provide different conditions at outlet like pressure outlet. In this case, we have considered outlet as outflow with weightage factor of 1.

Free surface: for case of open channel flow it is important to create free surface so the free surface boundary is assigned as symmetry.

Bed and sidewalls: bed, sidewalls and the groyne surface are considered as hydrodynamically smooth surfaces and as designated as wall.

Solution: Next step is to initialize the solution. Total number of iteration are always more than 500 and it is found that solution always gets converged in less than 500 iteration. The total run time for impermeable case is always found to be less than that for permeable case. Time step size taken is 0.05 sec for stability of the solution.
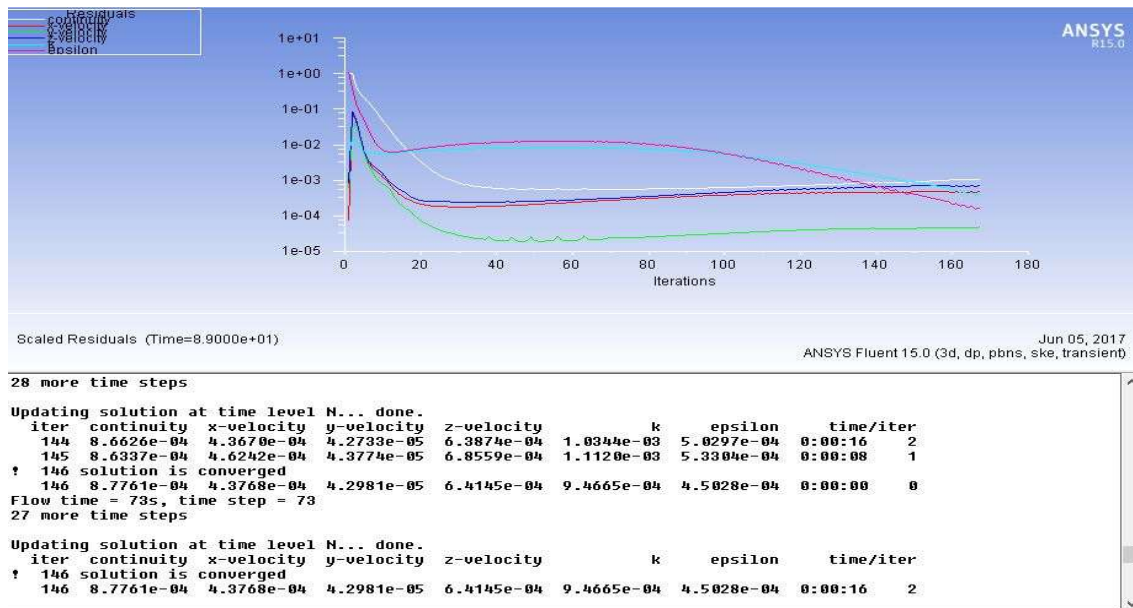
Figure 3.16 Solution Convergence in ANSYS Software

Chapter 4 NUMERICAL DATA

4.1 Software Output

From the series of 5 groyne, stable condition is always found beyond 4th groyne, so mainly studies focus around groyne 4 named as G4. Following few table now shows the variation of velocity near the tip of G4. Here V_{APP}= Velocity of approach to groyne field in m/s, V_{TE}= tip velocity at the G4 groyne obtained experimentally in m/s, V_{TN} = tip velocity at G4 groyne obtained numerically.

Table 4.1 Tip Velocity for M1 Model

S.No.	Z	Z/L	V_{APP}	V_{TE}	V_{TE}/V_{APP}	V_{TN}	V_{TN}/V_{APP}
1	18.250	0.608	0.350	0.260	0.743	0.235	0.671
2	18.500	0.617	0.350	0.280	0.800	0.278	0.794
3	18.750	0.625	0.350	0.300	0.857	0.326	0.933
4	19.000	0.633	0.350	0.280	0.800	0.265	0.757
5	19.250	0.642	0.350	0.300	0.857	0.290	0.829

Table 4.2 Tip Velocity for M2 Model

S.No.	Z	Z/L	V_{APP}	V_{TE}	V_{TE}/V_{APP}	V_{TN}	V_{NUM}/V_{APP}
1	18.250	0.608	0.350	0.220	0.629	0.201	0.575
2	18.500	0.617	0.350	0.280	0.800	0.318	0.907
3	18.750	0.625	0.350	0.260	0.743	0.254	0.724
4	19.000	0.633	0.350	0.250	0.714	0.225	0.643
5	19.250	0.642	0.350	0.230	0.657	0.205	0.586

Table 4.3 Tip Velocity for M3 Model

S.No.	Z	Z/L	V_{APP}	V_{TE}	V_{TE}/V_{APP}	V_{TN}	V_{NUM}/V_{APP}
1	18.250	0.608	0.350	0.265	0.757	0.265	0.757
2	18.500	0.617	0.350	0.260	0.743	0.268	0.764
3	18.750	0.625	0.350	0.255	0.729	0.270	0.772
4	19.000	0.633	0.350	0.243	0.694	0.246	0.703
5	19.250	0.642	0.350	0.240	0.686	0.241	0.689

Table 4.4 Tip Velocity for M4 Model

S.No.	Z	Z/L	V_{APP}	V_{TE}	V_{EXP}/V_{APP}	V_{TN}	V_{NUM}/V_{APP}
1	18.250	0.608	0.350	0.260	0.743	0.256	0.733
2	18.500	0.617	0.350	0.265	0.757	0.261	0.747
3	18.750	0.625	0.350	0.270	0.771	0.276	0.788
4	19.000	0.633	0.350	0.260	0.743	0.262	0.750
5	19.250	0.642	0.350	0.255	0.729	0.250	0.714

For comparing the various model a critical section is defined at 0.75 m from the tip of G4 groyne. Following table is for horizontal profile of velocity at critical section. Here X is measured across the flow from the protected bank. B is defined as total width of the channel. V_{CN} = velocity of flow at critical section.

Table 4.5 Horizontal Profile of Velocity at Critical Section

S.No.	MODEL	X	X/B	V_{APP}	V_{CN}	V_{CN}/V_{APP}
1	M1	0.556	0.111	0.350	0.172	0.492
2	M1	1.111	0.222	0.350	0.165	0.472
3	M1	2.222	0.444	0.350	0.336	0.961
4	M1	3.333	0.667	0.350	0.188	0.536
5	M1	4.444	0.889	0.350	0.152	0.434
6	M2	0.556	0.111	0.350	0.162	0.464
7	M2	1.111	0.222	0.350	0.326	0.931
8	M2	2.222	0.444	0.350	0.301	0.860
9	M2	3.333	0.667	0.350	0.165	0.472
10	M2	4.444	0.889	0.350	0.124	0.354
11	M3	0.556	0.111	0.350	0.168	0.480
12	M3	1.111	0.222	0.350	0.225	0.644
13	M3	2.222	0.444	0.350	0.153	0.437
14	M3	3.333	0.667	0.350	0.192	0.549
15	M3	4.444	0.889	0.350	0.201	0.574

16	M4	0.556	0.111	0.350	0.210	0.601
17	M4	1.111	0.222	0.350	0.168	0.479
18	M4	2.222	0.444	0.350	0.213	0.609
19	M4	3.333	0.667	0.350	0.186	0.531
20	M4	4.444	0.889	0.350	0.131	0.374

Following table is for the vertical profile at critical section. Y here shows point above the bottom of the channel. D defines total depth of the channel

Table 4.6 Vertical Profile of Velocity at Critical Section

S.No.	Model	Y	Y/D	V_{APP}	V_{CN}	V_{CN}/V_{APP}
1	M1	0.083	0.333	0.350	0.034	0.098
2	M1	0.111	0.444	0.350	0.119	0.340
3	M1	0.139	0.556	0.350	0.159	0.454
4	M1	0.167	0.667	0.350	0.183	0.522
5	M1	0.194	0.778	0.350	0.228	0.651
6	M1	0.222	0.889	0.350	0.267	0.764
7	M2	0.083	0.333	0.350	0.035	0.099
8	M2	0.111	0.444	0.350	0.128	0.366
9	M2	0.139	0.556	0.350	0.180	0.514
10	M2	0.167	0.667	0.350	0.207	0.593
11	M2	0.194	0.778	0.350	0.237	0.678
12	M2	0.222	0.889	0.350	0.274	0.782
13	M3	0.028	0.111	0.350	0.097	0.278
14	M3	0.056	0.222	0.350	0.124	0.355
15	M3	0.083	0.333	0.350	0.143	0.410
16	M3	0.111	0.444	0.350	0.162	0.463
17	M3	0.139	0.556	0.350	0.178	0.507
18	M3	0.167	0.667	0.350	0.199	0.568
19	M3	0.194	0.778	0.350	0.209	0.597
20	M3	0.222	0.889	0.350	0.227	0.648
21	M4	0.028	0.111	0.350	0.172	0.492

22	M4	0.056	0.222	0.350	0.204	0.584
23	M4	0.083	0.333	0.350	0.228	0.651
24	M4	0.111	0.444	0.350	0.243	0.696
25	M4	0.139	0.556	0.350	0.272	0.777
26	M4	0.167	0.667	0.350	0.290	0.828
27	M4	0.194	0.778	0.350	0.303	0.866
28	M4	0.222	0.889	0.350	0.316	0.903

Following table shows variation of turbulent kinetic Energy (TKE) at critical section.

Table 4.7 Variation of TKE at Critical Section

S.No.	Model	X	X/B	TKE(i)	TKE	TKE/TKE(i)
1	M1	0.000	0.000	0.023	0.028	1.229
2	M1	0.556	0.111	0.023	0.023	1.002
3	M1	1.111	0.222	0.023	0.023	1.010
4	M1	1.667	0.333	0.023	0.024	1.039
5	M1	2.222	0.444	0.023	0.028	1.198
6	M1	2.778	0.556	0.023	0.036	1.563
7	M1	3.333	0.667	0.023	0.034	1.463
8	M1	3.889	0.778	0.023	0.018	0.786
9	M1	4.444	0.889	0.023	0.012	0.519
10	M1	5.000	1.000	0.023	0.014	0.624
11	M2	0.000	0.000	0.023	0.028	1.229
12	M2	0.556	0.111	0.023	0.023	1.007
13	M2	1.111	0.222	0.023	0.024	1.027
14	M2	1.667	0.333	0.023	0.026	1.121
15	M2	2.222	0.444	0.023	0.033	1.448
16	M2	2.778	0.556	0.023	0.030	1.315
17	M2	3.333	0.667	0.023	0.029	1.244
18	M2	3.889	0.778	0.023	0.022	0.978
19	M2	4.444	0.889	0.023	0.012	0.537

20	M2	5.000	1.000	0.023	0.013	0.550
21	M3	0.000	0.000	0.023	0.029	1.251
22	M3	0.556	0.111	0.023	0.023	1.002
23	M3	1.111	0.222	0.023	0.023	1.005
24	M3	1.667	0.333	0.023	0.029	1.258
25	M3	2.222	0.444	0.023	0.025	1.106
26	M3	2.778	0.556	0.023	0.021	0.895
27	M3	3.333	0.667	0.023	0.022	0.969
28	M3	3.889	0.778	0.023	0.021	0.929
29	M3	4.444	0.889	0.023	0.020	0.874
30	M3	5.000	1.000	0.023	0.021	0.927
31	M4	0.000	0.000	0.023	0.029	1.260
32	M4	0.556	0.111	0.023	0.023	1.012
33	M4	1.111	0.222	0.023	0.023	0.985
34	M4	1.667	0.333	0.023	0.023	1.014
35	M4	2.222	0.444	0.023	0.029	1.256
36	M4	2.778	0.556	0.023	0.026	1.114
37	M4	3.333	0.667	0.023	0.024	1.030
38	M4	3.889	0.778	0.023	0.020	0.871
39	M4	4.444	0.889	0.023	0.020	0.867
40	M4	5.000	1.000	0.023	0.016	0.705

Following table shows the variation of velocity at different location varying wrt protected bank.

Table 4.8 Velocity Variation at X/B=0.8

S.No.	Model	Z	Z/L	V_{APP}	V_N	V_N/V_{APP}
1	M1	0.000	0.000	0.350	0.350	1.000
2	M1	3.333	0.111	0.350	0.361	1.031
3	M1	6.667	0.222	0.350	0.390	1.114
4	M1	10.000	0.333	0.350	0.359	1.026
5	M1	13.333	0.444	0.350	0.364	1.040

6	M1	16.667	0.556	0.350	0.371	1.060
7	M1	20.000	0.667	0.350	0.361	1.031
8	M1	23.333	0.778	0.350	0.369	1.054
9	M1	26.667	0.889	0.350	0.341	0.974
10	M1	30.000	1.000	0.350	0.319	0.911
11	M2	0.000	0.000	0.350	0.350	1.000
12	M2	3.333	0.111	0.350	0.371	1.060
13	M2	6.667	0.222	0.350	0.401	1.146
14	M2	10.000	0.333	0.350	0.361	1.031
15	M2	13.333	0.444	0.350	0.370	1.057
16	M2	16.667	0.556	0.350	0.377	1.077
17	M2	20.000	0.667	0.350	0.366	1.046
18	M2	23.333	0.778	0.350	0.379	1.083
19	M2	26.667	0.889	0.350	0.355	1.014
20	M2	30.000	1.000	0.350	0.301	0.860
21	M3	0.000	0.000	0.350	0.350	1.000
22	M3	3.333	0.111	0.350	0.357	1.020
23	M3	6.667	0.222	0.350	0.466	1.331
24	M3	10.000	0.333	0.350	0.401	1.146
25	M3	13.333	0.444	0.350	0.438	1.251
26	M3	16.667	0.556	0.350	0.399	1.140
27	M3	20.000	0.667	0.350	0.429	1.226
28	M3	23.333	0.778	0.350	0.386	1.103
29	M3	26.667	0.889	0.350	0.366	1.046
30	M3	30.000	1.000	0.350	0.317	0.906
31	M4	0.000	0.000	0.350	0.350	1.000
32	M4	3.333	0.111	0.350	0.343	0.980
33	M4	6.667	0.222	0.350	0.381	1.088
34	M4	10.000	0.333	0.350	0.344	0.982
35	M4	13.333	0.444	0.350	0.355	1.016
36	M4	16.667	0.556	0.350	0.354	1.010
37	M4	20.000	0.667	0.350	0.364	1.039

38	M4	23.333	0.778	0.350	0.341	0.974
39	M4	26.667	0.889	0.350	0.355	1.014
40	M4	30.000	1.000	0.350	0.301	0.860

Table 4.9 Velocity Variation at X/B=0.7

S.No.	Model	Z	Z/L	Vapp	Vnum	Vnum/Vapp
1	M1	0.000	0.000	0.350	0.350	1.000
2	M1	3.333	0.111	0.350	0.369	1.054
3	M1	6.667	0.222	0.350	0.382	1.090
4	M1	10.000	0.333	0.350	0.358	1.021
5	M1	13.333	0.444	0.350	0.373	1.067
6	M1	16.667	0.556	0.350	0.361	1.031
7	M1	20.000	0.667	0.350	0.369	1.055
8	M1	23.333	0.778	0.350	0.359	1.026
9	M1	26.667	0.889	0.350	0.345	0.986
10	M1	30.000	1.000	0.350	0.333	0.951
11	M2	0.000	0.000	0.350	0.350	1.000
12	M2	3.333	0.111	0.350	0.379	1.083
13	M2	6.667	0.222	0.350	0.413	1.181
14	M2	10.000	0.333	0.350	0.350	1.000
15	M2	13.333	0.444	0.350	0.409	1.169
16	M2	16.667	0.556	0.350	0.355	1.014
17	M2	20.000	0.667	0.350	0.401	1.145
18	M2	23.333	0.778	0.350	0.351	1.002
19	M2	26.667	0.889	0.350	0.367	1.049
20	M2	30.000	1.000	0.350	0.311	0.889
21	M3	0.000	0.000	0.350	0.350	1.000
22	M3	3.333	0.111	0.350	0.361	1.031
23	M3	6.667	0.222	0.350	0.433	1.236
24	M3	10.000	0.333	0.350	0.384	1.098
25	M3	13.333	0.444	0.350	0.424	1.212
26	M3	16.667	0.556	0.350	0.403	1.150

27	M3	20.000	0.667	0.350	0.416	1.188
28	M3	23.333	0.778	0.350	0.386	1.102
29	M3	26.667	0.889	0.350	0.381	1.088
30	M3	30.000	1.000	0.350	0.312	0.891
31	M4	0.000	0.000	0.350	0.350	1.000
32	M4	3.333	0.111	0.350	0.361	1.031
33	M4	6.667	0.222	0.350	0.410	1.171
34	M4	10.000	0.333	0.350	0.361	1.031
35	M4	13.333	0.444	0.350	0.385	1.099
36	M4	16.667	0.556	0.350	0.346	0.990
37	M4	20.000	0.667	0.350	0.399	1.140
38	M4	23.333	0.778	0.350	0.365	1.042
39	M4	26.667	0.889	0.350	0.341	0.974
40	M4	30.000	1.000	0.350	0.311	0.889

Table 4.10 Velocity Variation at X/B=0.6

S.No.	Model	Z	Z/L	Vapp	Vnum	Vnum/Vapp
1	M1	0.000	0.000	0.350	0.350	1.000
2	M1	3.333	0.111	0.350	0.391	1.117
3	M1	6.667	0.222	0.350	0.455	1.300
4	M1	10.000	0.333	0.350	0.399	1.140
5	M1	13.333	0.444	0.350	0.432	1.235
6	M1	16.667	0.556	0.350	0.410	1.171
7	M1	20.000	0.667	0.350	0.429	1.226
8	M1	23.333	0.778	0.350	0.430	1.229
9	M1	26.667	0.889	0.350	0.355	1.014
10	M1	30.000	1.000	0.350	0.327	0.934
11	M2	0.000	0.000	0.350	0.350	1.000
12	M2	3.333	0.111	0.350	0.382	1.091
13	M2	6.667	0.222	0.350	0.526	1.504
14	M2	10.000	0.333	0.350	0.467	1.333
15	M2	13.333	0.444	0.350	0.500	1.429

16	M2	16.667	0.556	0.350	0.448	1.280
17	M2	20.000	0.667	0.350	0.488	1.395
18	M2	23.333	0.778	0.350	0.472	1.348
19	M2	26.667	0.889	0.350	0.361	1.031
20	M2	30.000	1.000	0.350	0.323	0.923
21	M3	0.000	0.000	0.350	0.350	1.000
22	M3	3.333	0.111	0.350	0.361	1.031
23	M3	6.667	0.222	0.350	0.312	0.891
24	M3	10.000	0.333	0.350	0.342	0.977
25	M3	13.333	0.444	0.350	0.256	0.731
26	M3	16.667	0.556	0.350	0.289	0.826
27	M3	20.000	0.667	0.350	0.273	0.780
28	M3	23.333	0.778	0.350	0.296	0.846
29	M3	26.667	0.889	0.350	0.231	0.660
30	M3	30.000	1.000	0.350	0.222	0.634
31	M4	0.000	0.000	0.350	0.350	1.000
32	M4	3.333	0.111	0.350	0.368	1.051
33	M4	6.667	0.222	0.350	0.423	1.209
34	M4	10.000	0.333	0.350	0.386	1.103
35	M4	13.333	0.444	0.350	0.411	1.174
36	M4	16.667	0.556	0.350	0.391	1.117
37	M4	20.000	0.667	0.350	0.399	1.140
38	M4	23.333	0.778	0.350	0.412	1.177
39	M4	26.667	0.889	0.350	0.339	0.969
40	M4	30.000	1.000	0.350	0.328	0.937

Table 4.11 Velocity Variation at X/B=0.5

S.No.	Model	Z	Z/L	Vapp	Vnum	Vnum/Vapp
1	M1	0.000	0.000	0.350	0.350	1.000
2	M1	3.333	0.111	0.350	0.429	1.226
3	M1	6.667	0.222	0.350	0.533	1.523
4	M1	10.000	0.333	0.350	0.427	1.219

5	M1	13.333	0.444	0.350	0.446	1.274
6	M1	16.667	0.556	0.350	0.401	1.146
7	M1	20.000	0.667	0.350	0.449	1.283
8	M1	23.333	0.778	0.350	0.396	1.133
9	M1	26.667	0.889	0.350	0.341	0.974
10	M1	30.000	1.000	0.350	0.243	0.694
11	M2	0.000	0.000	0.350	0.350	1.000
12	M2	3.333	0.111	0.350	0.403	1.151
13	M2	6.667	0.222	0.350	0.412	1.177
14	M2	10.000	0.333	0.350	0.329	0.940
15	M2	13.333	0.444	0.350	0.359	1.026
16	M2	16.667	0.556	0.350	0.324	0.926
17	M2	20.000	0.667	0.350	0.349	0.997
18	M2	23.333	0.778	0.350	0.321	0.917
19	M2	26.667	0.889	0.350	0.322	0.920
20	M2	30.000	1.000	0.350	0.231	0.660
21	M3	0.000	0.000	0.350	0.350	1.000
22	M3	3.333	0.111	0.350	0.256	0.731
23	M3	6.667	0.222	0.350	0.186	0.531
24	M3	10.000	0.333	0.350	0.153	0.437
25	M3	13.333	0.444	0.350	0.163	0.466
26	M3	16.667	0.556	0.350	0.153	0.437
27	M3	20.000	0.667	0.350	0.137	0.391
28	M3	23.333	0.778	0.350	0.142	0.406
29	M3	26.667	0.889	0.350	0.152	0.434
30	M3	30.000	1.000	0.350	0.120	0.343
31	M4	0.000	0.000	0.350	0.350	1.000
32	M4	3.333	0.111	0.350	0.301	0.860
33	M4	6.667	0.222	0.350	0.246	0.701
34	M4	10.000	0.333	0.350	0.256	0.732
35	M4	13.333	0.444	0.350	0.288	0.823
36	M4	16.667	0.556	0.350	0.232	0.663

37	M4	20.000	0.667	0.350	0.276	0.789
38	M4	23.333	0.778	0.350	0.258	0.737
39	M4	26.667	0.889	0.350	0.232	0.663
40	M4	30.000	1.000	0.350	0.201	0.574

Table 4.12 Velocity Variation at X/B=0.4

S.No.	Model	Z	Z/L	Vapp	Vnum	Vnum/Vapp
1	M1	0.000	0.000	0.350	0.350	1.000
2	M1	3.333	0.111	0.350	0.281	0.803
3	M1	6.667	0.222	0.350	0.329	0.940
4	M1	10.000	0.333	0.350	0.276	0.789
5	M1	13.333	0.444	0.350	0.318	0.909
6	M1	16.667	0.556	0.350	0.263	0.751
7	M1	20.000	0.667	0.350	0.313	0.894
8	M1	23.333	0.778	0.350	0.283	0.809
9	M1	26.667	0.889	0.350	0.301	0.860
10	M1	30.000	1.000	0.350	0.261	0.746
11	M2	0.000	0.000	0.350	0.350	1.000
12	M2	3.333	0.111	0.350	0.286	0.817
13	M2	6.667	0.222	0.350	0.277	0.793
14	M2	10.000	0.333	0.350	0.227	0.649
15	M2	13.333	0.444	0.350	0.268	0.766
16	M2	16.667	0.556	0.350	0.227	0.649
17	M2	20.000	0.667	0.350	0.257	0.734
18	M2	23.333	0.778	0.350	0.213	0.609
19	M2	26.667	0.889	0.350	0.249	0.711
20	M2	30.000	1.000	0.350	0.238	0.680
21	M3	0.000	0.000	0.350	0.350	1.000
22	M3	3.333	0.111	0.350	0.197	0.563
23	M3	6.667	0.222	0.350	0.123	0.352
24	M3	10.000	0.333	0.350	0.121	0.347
25	M3	13.333	0.444	0.350	0.134	0.383

26	M3	16.667	0.556	0.350	0.122	0.349
27	M3	20.000	0.667	0.350	0.131	0.373
28	M3	23.333	0.778	0.350	0.125	0.357
29	M3	26.667	0.889	0.350	0.133	0.380
30	M3	30.000	1.000	0.350	0.212	0.606
31	M4	0.000	0.000	0.350	0.350	1.000
32	M4	3.333	0.111	0.350	0.204	0.584
33	M4	6.667	0.222	0.350	0.162	0.463
34	M4	10.000	0.333	0.350	0.143	0.409
35	M4	13.333	0.444	0.350	0.173	0.494
36	M4	16.667	0.556	0.350	0.137	0.391
37	M4	20.000	0.667	0.350	0.173	0.494
38	M4	23.333	0.778	0.350	0.136	0.389
39	M4	26.667	0.889	0.350	0.171	0.489
40	M4	30.000	1.000	0.350	0.238	0.680

Table 4.13 Velocity Variation at X/B=0.3

S.No.	Model	Z	Z/L	Vapp	Vnum	Vnum/Vapp
1	M1	0.000	0.000	0.350	0.350	1.000
2	M1	3.333	0.111	0.350	0.201	0.574
3	M1	6.667	0.222	0.350	0.053	0.151
4	M1	10.000	0.333	0.350	0.086	0.246
5	M1	13.333	0.444	0.350	0.055	0.157
6	M1	16.667	0.556	0.350	0.081	0.231
7	M1	20.000	0.667	0.350	0.061	0.174
8	M1	23.333	0.778	0.350	0.079	0.226
9	M1	26.667	0.889	0.350	0.049	0.140
10	M1	30.000	1.000	0.350	0.190	0.543
11	M2	0.000	0.000	0.350	0.350	1.000
12	M2	3.333	0.111	0.350	0.194	0.554
13	M2	6.667	0.222	0.350	0.083	0.237
14	M2	10.000	0.333	0.350	0.101	0.289

15	M2	13.333	0.444	0.350	0.091	0.260
16	M2	16.667	0.556	0.350	0.110	0.314
17	M2	20.000	0.667	0.350	0.089	0.254
18	M2	23.333	0.778	0.350	0.099	0.283
19	M2	26.667	0.889	0.350	0.111	0.317
20	M2	30.000	1.000	0.350	0.210	0.600
21	M3	0.000	0.000	0.350	0.350	1.000
22	M3	3.333	0.111	0.350	0.240	0.686
23	M3	6.667	0.222	0.350	0.139	0.397
24	M3	10.000	0.333	0.350	0.151	0.431
25	M3	13.333	0.444	0.350	0.127	0.363
26	M3	16.667	0.556	0.350	0.137	0.391
27	M3	20.000	0.667	0.350	0.126	0.360
28	M3	23.333	0.778	0.350	0.134	0.383
29	M3	26.667	0.889	0.350	0.173	0.494
30	M3	30.000	1.000	0.350	0.234	0.669
31	M4	0.000	0.000	0.350	0.350	1.000
32	M4	3.333	0.111	0.350	0.224	0.640
33	M4	6.667	0.222	0.350	0.117	0.334
34	M4	10.000	0.333	0.350	0.142	0.406
35	M4	13.333	0.444	0.350	0.147	0.420
36	M4	16.667	0.556	0.350	0.161	0.460
37	M4	20.000	0.667	0.350	0.122	0.347
38	M4	23.333	0.778	0.350	0.144	0.413
39	M4	26.667	0.889	0.350	0.201	0.574
40	M4	30.000	1.000	0.350	0.256	0.731

Following tables shows the maximum values of few parameters and their respective location wrt G4 groyne tip. Here V(max)= maximum velocity in m/s, Z(T)=distance along the direction of flow from G4 tip in m, X(T)=distance across the flow from G4 tip in m, Y=height above the bottom of the channel in m

Table 4.14 Maximum Velocity And Its Location

S.No.	Model	V(max)	Z(T)	X(T)	Y
1	M1	0.691	0.712	0.275	0.216
2	M2	0.639	0.446	0.271	0.221
3	M3	0.501	0.148	0.157	0.211
4	M4	0.543	0.312	0.198	0.208

Table 4.15 Maximum Shear And Its Location

S.No.	Model	shear(max)	Z(T)	X(T)
1	M1	1.975	0.627	0.36
2	M2	1.513	0.416	0.18
3	M3	0.547	0.126	0.09
4	M4	0.783	0.312	0.11

Table 4.16 Maximum TKE And Its Location

S.No.	Model	TKE(max)	Z(T)	X(T)	Y
1	M1	0.148	0.194	0.361	0.112
2	M2	0.122	0.133	0.199	0.124
3	M3	0.089	0.064	0.112	0.165
4	M4	0.105	0.109	0.174	0.132

Following table shows the variation of shear stress on different location wrt the protected bank. Here τ_0 = nominal shear stress on bed when there is no groynes are placed in the flow field. τ =shear stress on the bed when groynes are placed in the flow field.

Table 4.17 Variation of Shear Stress at X/B=0.8

S.No.	Model	Z	Z/L	τ_0	τ	τ/τ_0
1	M1	0.000	0.000	0.211	0.211	1.000
2	M1	3.333	0.111	0.211	0.229	1.085
3	M1	6.667	0.222	0.211	0.235	1.114
4	M1	10.000	0.333	0.211	0.256	1.213

5	M1	13.333	0.444	0.211	0.246	1.166
6	M1	16.667	0.556	0.211	0.271	1.284
7	M1	20.000	0.667	0.211	0.261	1.237
8	M1	23.333	0.778	0.211	0.263	1.246
9	M1	26.667	0.889	0.211	0.243	1.150
10	M1	30.000	1.000	0.211	0.194	0.917
11	M2	0.000	0.000	0.211	0.211	1.000
12	M2	3.333	0.111	0.211	0.214	1.013
13	M2	6.667	0.222	0.211	0.251	1.190
14	M2	10.000	0.333	0.211	0.261	1.237
15	M2	13.333	0.444	0.211	0.277	1.312
16	M2	16.667	0.556	0.211	0.263	1.246
17	M2	20.000	0.667	0.211	0.283	1.341
18	M2	23.333	0.778	0.211	0.283	1.341
19	M2	26.667	0.889	0.211	0.244	1.154
20	M2	30.000	1.000	0.211	0.214	1.015
21	M3	0.000	0.000	0.211	0.211	1.000
22	M3	3.333	0.111	0.211	0.212	1.005
23	M3	6.667	0.222	0.211	0.338	1.602
24	M3	10.000	0.333	0.211	0.315	1.493
25	M3	13.333	0.444	0.211	0.323	1.531
26	M3	16.667	0.556	0.211	0.295	1.398
27	M3	20.000	0.667	0.211	0.314	1.488
28	M3	23.333	0.778	0.211	0.301	1.427
29	M3	26.667	0.889	0.211	0.216	1.024
30	M3	30.000	1.000	0.211	0.199	0.944
31	M4	0.000	0.000	0.211	0.211	1.000
32	M4	3.333	0.111	0.211	0.234	1.109
33	M4	6.667	0.222	0.211	0.244	1.156
34	M4	10.000	0.333	0.211	0.263	1.246
35	M4	13.333	0.444	0.211	0.251	1.190
36	M4	16.667	0.556	0.211	0.253	1.199

S.No.	Model	Z	Z/L	τ_0	τ	τ/τ_0
37	M4	20.000	0.667	0.211	0.271	1.284
38	M4	23.333	0.778	0.211	0.253	1.199
39	M4	26.667	0.889	0.211	0.245	1.162
40	M4	30.000	1.000	0.211	0.205	0.974

Table 4.18 variation of shear stress at X/B=0.7

S.No.	Model	Z	Z/L	τ_0	τ	τ/τ_0
1	M1	0.000	0.000	0.211	0.211	1.000
2	M1	3.333	0.111	0.211	0.222	1.054
3	M1	6.667	0.222	0.211	0.286	1.355
4	M1	10.000	0.333	0.211	0.291	1.379
5	M1	13.333	0.444	0.211	0.263	1.246
6	M1	16.667	0.556	0.211	0.281	1.332
7	M1	20.000	0.667	0.211	0.287	1.360
8	M1	23.333	0.778	0.211	0.273	1.294
9	M1	26.667	0.889	0.211	0.256	1.214
10	M1	30.000	1.000	0.211	0.200	0.946
11	M2	0.000	0.000	0.211	0.211	1.000
12	M2	3.333	0.111	0.211	0.221	1.047
13	M2	6.667	0.222	0.211	0.321	1.521
14	M2	10.000	0.333	0.211	0.311	1.473
15	M2	13.333	0.444	0.211	0.320	1.517
16	M2	16.667	0.556	0.211	0.291	1.379
17	M2	20.000	0.667	0.211	0.296	1.404
18	M2	23.333	0.778	0.211	0.297	1.408
19	M2	26.667	0.889	0.211	0.231	1.096
20	M2	30.000	1.000	0.211	0.206	0.975
21	M3	0.000	0.000	0.211	0.211	1.000
22	M3	3.333	0.111	0.211	0.243	1.152
23	M3	6.667	0.222	0.211	0.369	1.749
24	M3	10.000	0.333	0.211	0.351	1.664
25	M3	13.333	0.444	0.211	0.367	1.739

26	M3	16.667	0.556	0.211	0.331	1.569
27	M3	20.000	0.667	0.211	0.349	1.654
28	M3	23.333	0.778	0.211	0.329	1.559
29	M3	26.667	0.889	0.211	0.281	1.332
30	M3	30.000	1.000	0.211	0.197	0.932
31	M4	0.000	0.000	0.211	0.211	1.000
32	M4	3.333	0.111	0.211	0.233	1.103
33	M4	6.667	0.222	0.211	0.324	1.536
34	M4	10.000	0.333	0.211	0.331	1.569
35	M4	13.333	0.444	0.211	0.341	1.616
36	M4	16.667	0.556	0.211	0.310	1.469
37	M4	20.000	0.667	0.211	0.318	1.507
38	M4	23.333	0.778	0.211	0.311	1.474
39	M4	26.667	0.889	0.211	0.242	1.145
40	M4	30.000	1.000	0.211	0.209	0.989

Table 4.19 Variation of Shear Stress at X/B=0.6

S.No.	Model	Z	Z/L	τ_0	τ	τ/τ_0
1	M1	0.000	0.000	0.211	0.211	1.000
2	M1	3.333	0.111	0.211	0.210	0.997
3	M1	6.667	0.222	0.211	0.372	1.764
4	M1	10.000	0.333	0.211	0.350	1.658
5	M1	13.333	0.444	0.211	0.327	1.550
6	M1	16.667	0.556	0.211	0.351	1.664
7	M1	20.000	0.667	0.211	0.322	1.526
8	M1	23.333	0.778	0.211	0.311	1.474
9	M1	26.667	0.889	0.211	0.303	1.436
10	M1	30.000	1.000	0.211	0.253	1.199
11	M2	0.000	0.000	0.211	0.211	1.000
12	M2	3.333	0.111	0.211	0.251	1.190
13	M2	6.667	0.222	0.211	0.419	1.986
14	M2	10.000	0.333	0.211	0.379	1.796

15	M2	13.333	0.444	0.211	0.411	1.948
16	M2	16.667	0.556	0.211	0.370	1.754
17	M2	20.000	0.667	0.211	0.394	1.867
18	M2	23.333	0.778	0.211	0.367	1.739
19	M2	26.667	0.889	0.211	0.322	1.526
20	M2	30.000	1.000	0.211	0.288	1.365
21	M3	0.000	0.000	0.211	0.211	1.000
22	M3	3.333	0.111	0.211	0.243	1.152
23	M3	6.667	0.222	0.211	0.227	1.076
24	M3	10.000	0.333	0.211	0.208	0.986
25	M3	13.333	0.444	0.211	0.218	1.033
26	M3	16.667	0.556	0.211	0.192	0.910
27	M3	20.000	0.667	0.211	0.211	1.000
28	M3	23.333	0.778	0.211	0.201	0.953
29	M3	26.667	0.889	0.211	0.183	0.867
30	M3	30.000	1.000	0.211	0.219	1.038
31	M4	0.000	0.000	0.211	0.211	1.000
32	M4	3.333	0.111	0.211	0.249	1.180
33	M4	6.667	0.222	0.211	0.319	1.512
34	M4	10.000	0.333	0.211	0.273	1.294
35	M4	13.333	0.444	0.211	0.303	1.436
36	M4	16.667	0.556	0.211	0.267	1.265
37	M4	20.000	0.667	0.211	0.281	1.332
38	M4	23.333	0.778	0.211	0.253	1.199
39	M4	26.667	0.889	0.211	0.241	1.142
40	M4	30.000	1.000	0.211	0.222	1.052

Table 4.20 Variation of Shear Stress at X/B=0.5

S.No.	Model	Z	Z/L	τ_0	τ	τ/τ_0
1	M1	0.000	0.000	0.211	0.211	1.000
2	M1	3.333	0.111	0.211	0.275	1.303
3	M1	6.667	0.222	0.211	0.538	2.550

4	M1	10.000	0.333	0.211	0.411	1.948
5	M1	13.333	0.444	0.211	0.486	2.303
6	M1	16.667	0.556	0.211	0.412	1.952
7	M1	20.000	0.667	0.211	0.453	2.147
8	M1	23.333	0.778	0.211	0.337	1.598
9	M1	26.667	0.889	0.211	0.219	1.038
10	M1	30.000	1.000	0.211	0.191	0.906
11	M2	0.000	0.000	0.211	0.211	1.000
12	M2	3.333	0.111	0.211	0.200	0.946
13	M2	6.667	0.222	0.211	0.356	1.689
14	M2	10.000	0.333	0.211	0.338	1.602
15	M2	13.333	0.444	0.211	0.236	1.120
16	M2	16.667	0.556	0.211	0.252	1.195
17	M2	20.000	0.667	0.211	0.348	1.649
18	M2	23.333	0.778	0.211	0.288	1.365
19	M2	26.667	0.889	0.211	0.223	1.058
20	M2	30.000	1.000	0.211	0.198	0.938
21	M3	0.000	0.000	0.211	0.211	1.000
22	M3	3.333	0.111	0.211	0.231	1.095
23	M3	6.667	0.222	0.211	0.151	0.716
24	M3	10.000	0.333	0.211	0.184	0.872
25	M3	13.333	0.444	0.211	0.146	0.692
26	M3	16.667	0.556	0.211	0.174	0.825
27	M3	20.000	0.667	0.211	0.141	0.668
28	M3	23.333	0.778	0.211	0.159	0.754
29	M3	26.667	0.889	0.211	0.178	0.844
30	M3	30.000	1.000	0.211	0.201	0.954
31	M4	0.000	0.000	0.211	0.211	1.000
32	M4	3.333	0.111	0.211	0.243	1.152
33	M4	6.667	0.222	0.211	0.235	1.114
34	M4	10.000	0.333	0.211	0.376	1.782
35	M4	13.333	0.444	0.211	0.206	0.975

36	M4	16.667	0.556	0.211	0.281	1.332
37	M4	20.000	0.667	0.211	0.367	1.739
38	M4	23.333	0.778	0.211	0.251	1.190
39	M4	26.667	0.889	0.211	0.209	0.991
40	M4	30.000	1.000	0.211	0.212	1.006

Table 4.21 Variation of Shear Stress at X/B=0.4

S.No.	Model	Z	Z/L	τ_0	τ	τ/τ_0
1	M1	0.000	0.000	0.211	0.211	1.000
2	M1	3.333	0.111	0.211	0.251	1.190
3	M1	6.667	0.222	0.211	0.357	1.692
4	M1	10.000	0.333	0.211	0.286	1.355
5	M1	13.333	0.444	0.211	0.326	1.545
6	M1	16.667	0.556	0.211	0.273	1.294
7	M1	20.000	0.667	0.211	0.305	1.445
8	M1	23.333	0.778	0.211	0.261	1.237
9	M1	26.667	0.889	0.211	0.208	0.984
10	M1	30.000	1.000	0.211	0.210	0.996
11	M2	0.000	0.000	0.211	0.211	1.000
12	M2	3.333	0.111	0.211	0.237	1.123
13	M2	6.667	0.222	0.211	0.253	1.199
14	M2	10.000	0.333	0.211	0.210	0.995
15	M2	13.333	0.444	0.211	0.233	1.104
16	M2	16.667	0.556	0.211	0.213	1.010
17	M2	20.000	0.667	0.211	0.201	0.953
18	M2	23.333	0.778	0.211	0.222	1.052
19	M2	26.667	0.889	0.211	0.202	0.958
20	M2	30.000	1.000	0.211	0.214	1.014
21	M3	0.000	0.000	0.211	0.211	1.000
22	M3	3.333	0.111	0.211	0.201	0.953
23	M3	6.667	0.222	0.211	0.179	0.848
24	M3	10.000	0.333	0.211	0.142	0.673

25	M3	13.333	0.444	0.211	0.169	0.801
26	M3	16.667	0.556	0.211	0.134	0.635
27	M3	20.000	0.667	0.211	0.171	0.810
28	M3	23.333	0.778	0.211	0.139	0.659
29	M3	26.667	0.889	0.211	0.177	0.839
30	M3	30.000	1.000	0.211	0.211	0.999
31	M4	0.000	0.000	0.211	0.211	1.000
32	M4	3.333	0.111	0.211	0.217	1.028
33	M4	6.667	0.222	0.211	0.238	1.127
34	M4	10.000	0.333	0.211	0.179	0.848
35	M4	13.333	0.444	0.211	0.202	0.957
36	M4	16.667	0.556	0.211	0.170	0.806
37	M4	20.000	0.667	0.211	0.183	0.867
38	M4	23.333	0.778	0.211	0.211	1.000
39	M4	26.667	0.889	0.211	0.207	0.980
40	M4	30.000	1.000	0.211	0.231	1.095

Table 4.22 Variation of Shear Stress at X/B=0.3

S.No.	Model	Z	Z/L	τ_0	τ	τ/τ_0
1	M1	0.000	0.000	0.211	0.211	1.000
2	M1	3.333	0.111	0.211	0.213	1.009
3	M1	6.667	0.222	0.211	0.126	0.597
4	M1	10.000	0.333	0.211	0.093	0.441
5	M1	13.333	0.444	0.211	0.119	0.564
6	M1	16.667	0.556	0.211	0.086	0.408
7	M1	20.000	0.667	0.211	0.120	0.569
8	M1	23.333	0.778	0.211	0.092	0.436
9	M1	26.667	0.889	0.211	0.156	0.739
10	M1	30.000	1.000	0.211	0.211	1.001
11	M2	0.000	0.000	0.211	0.211	1.000
12	M2	3.333	0.111	0.211	0.186	0.882
13	M2	6.667	0.222	0.211	0.143	0.678

14	M2	10.000	0.333	0.211	0.101	0.479
15	M2	13.333	0.444	0.211	0.121	0.573
16	M2	16.667	0.556	0.211	0.100	0.474
17	M2	20.000	0.667	0.211	0.137	0.649
18	M2	23.333	0.778	0.211	0.111	0.526
19	M2	26.667	0.889	0.211	0.170	0.803
20	M2	30.000	1.000	0.211	0.217	1.029
21	M3	0.000	0.000	0.211	0.211	1.000
22	M3	3.333	0.111	0.211	0.203	0.962
23	M3	6.667	0.222	0.211	0.181	0.858
24	M3	10.000	0.333	0.211	0.138	0.654
25	M3	13.333	0.444	0.211	0.175	0.829
26	M3	16.667	0.556	0.211	0.141	0.668
27	M3	20.000	0.667	0.211	0.169	0.801
28	M3	23.333	0.778	0.211	0.155	0.735
29	M3	26.667	0.889	0.211	0.191	0.904
30	M3	30.000	1.000	0.211	0.218	1.031
31	M4	0.000	0.000	0.211	0.211	1.000
32	M4	3.333	0.111	0.211	0.194	0.919
33	M4	6.667	0.222	0.211	0.161	0.763
34	M4	10.000	0.333	0.211	0.120	0.569
35	M4	13.333	0.444	0.211	0.131	0.621
36	M4	16.667	0.556	0.211	0.118	0.561
37	M4	20.000	0.667	0.211	0.159	0.754
38	M4	23.333	0.778	0.211	0.134	0.635
39	M4	26.667	0.889	0.211	0.194	0.921
40	M4	30.000	1.000	0.211	0.233	1.106

4.2 Software Plots
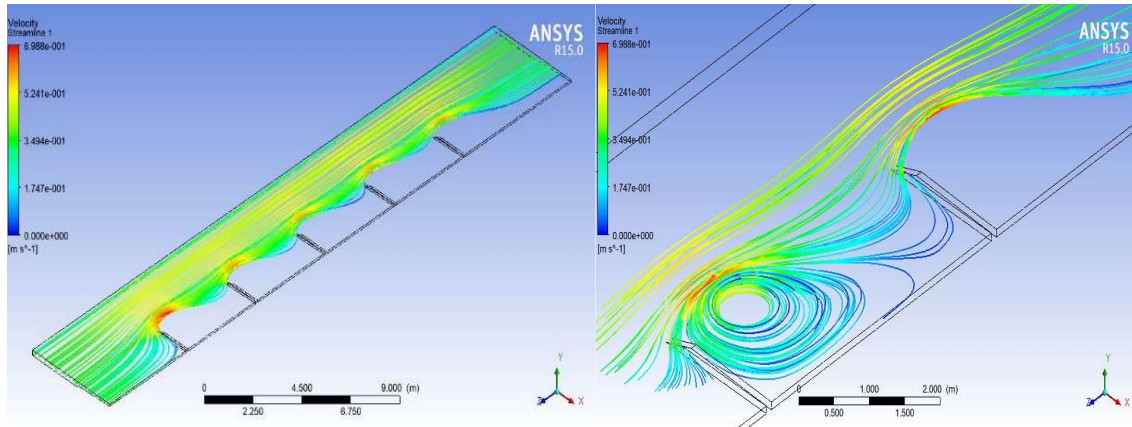
Figure 4.1 Streamline for M1 Model
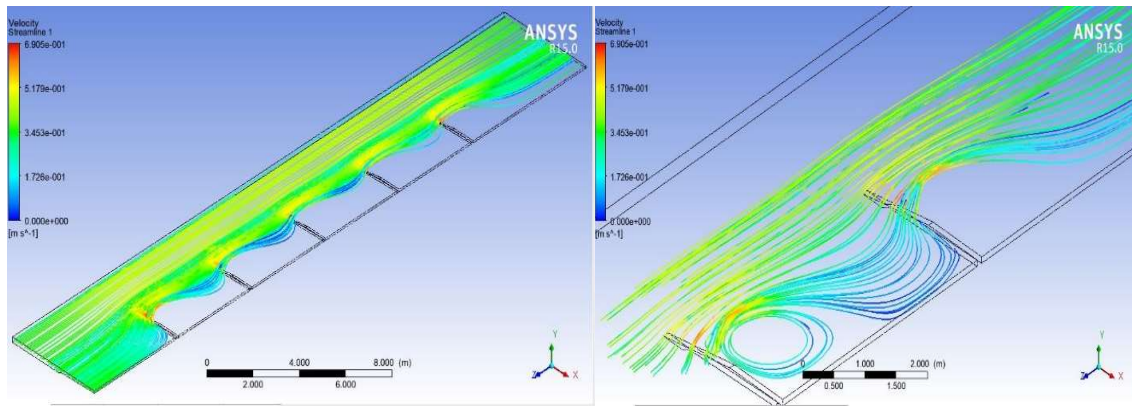
Figure 4.2 Streamline for M2 Model
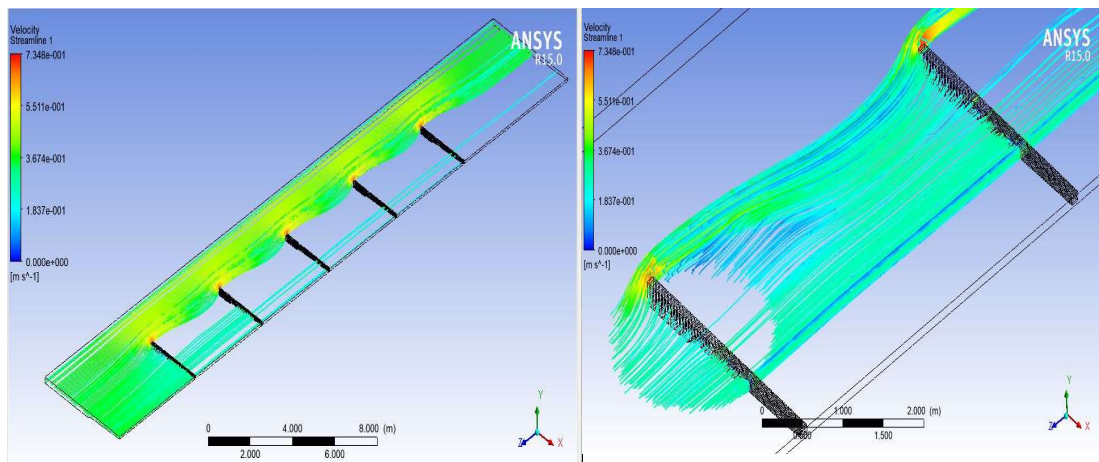
Figure 4.3 Streamline for M3 Model
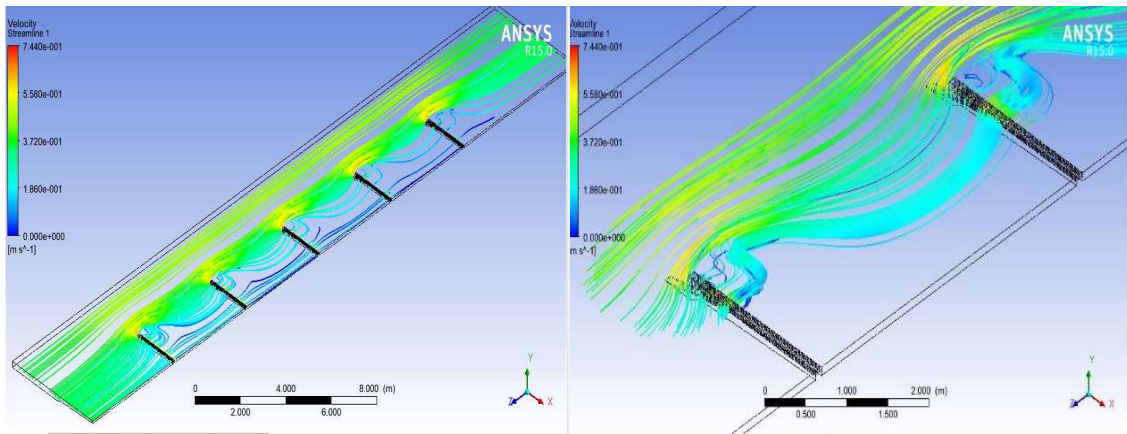
Figure 4.4 Streamline for M4 Model
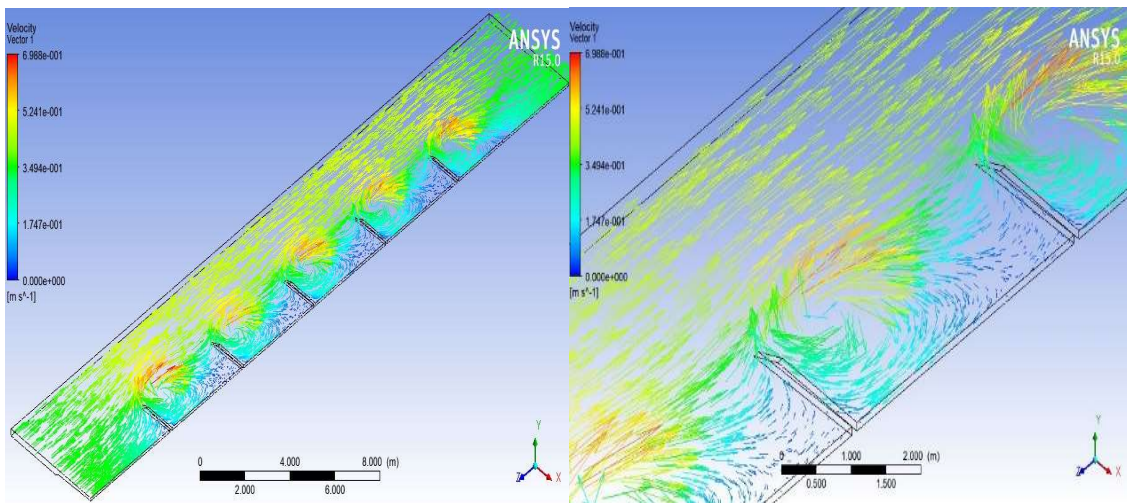
Figure 4.5 Velocity Vectors for M1 Model
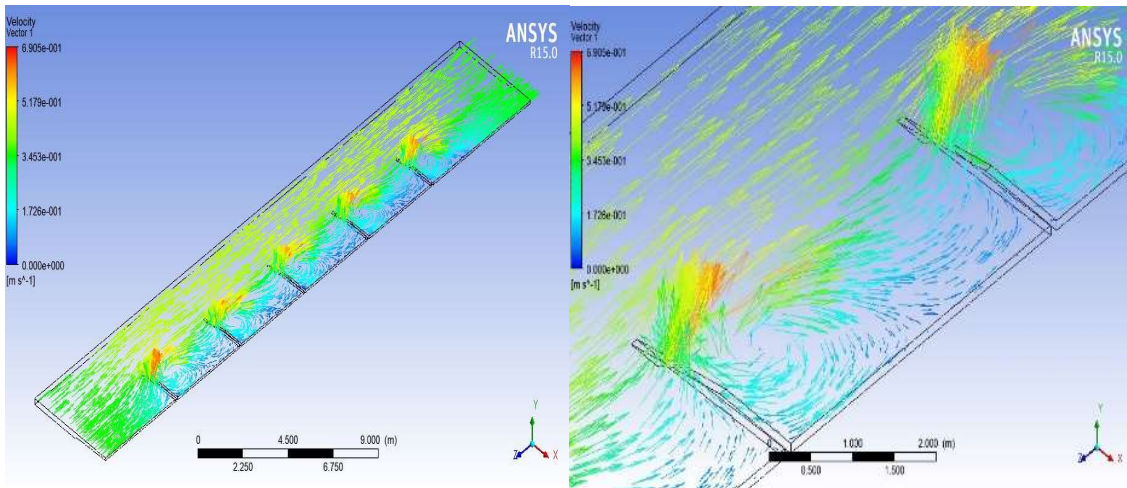
Figure 4.6 Velocity Vectors for M2 Model
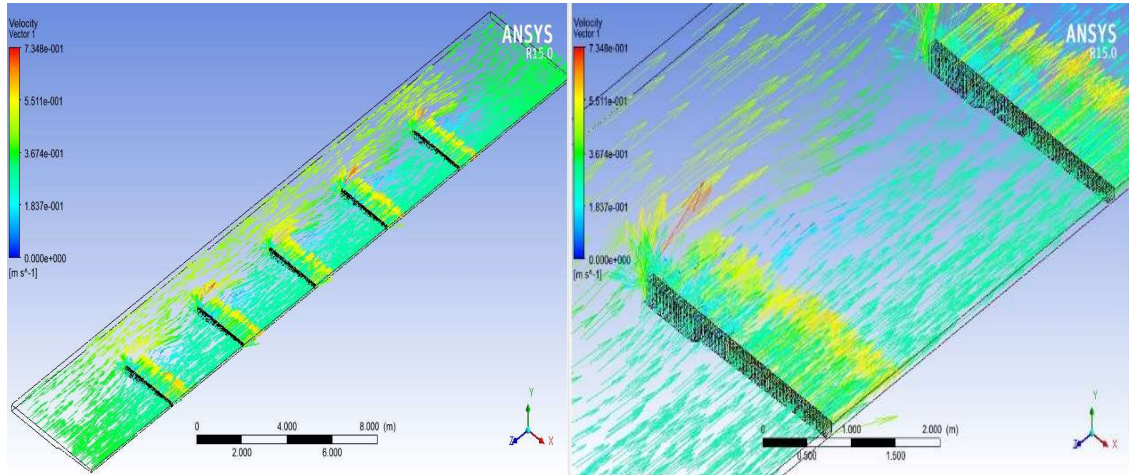
Figure 4.7 Velocity Vectors for M3 Model
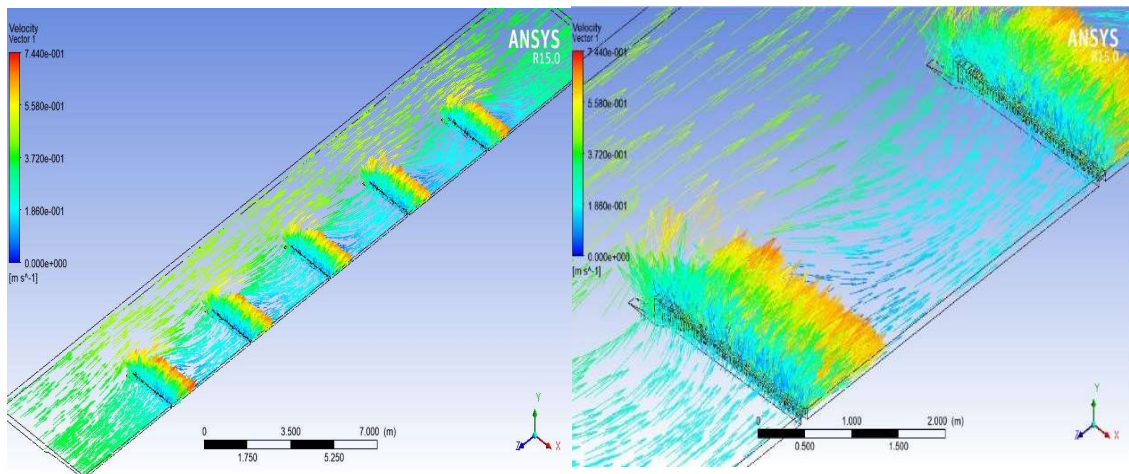
Figure 4.8 Velocity Vectors for M4 Model
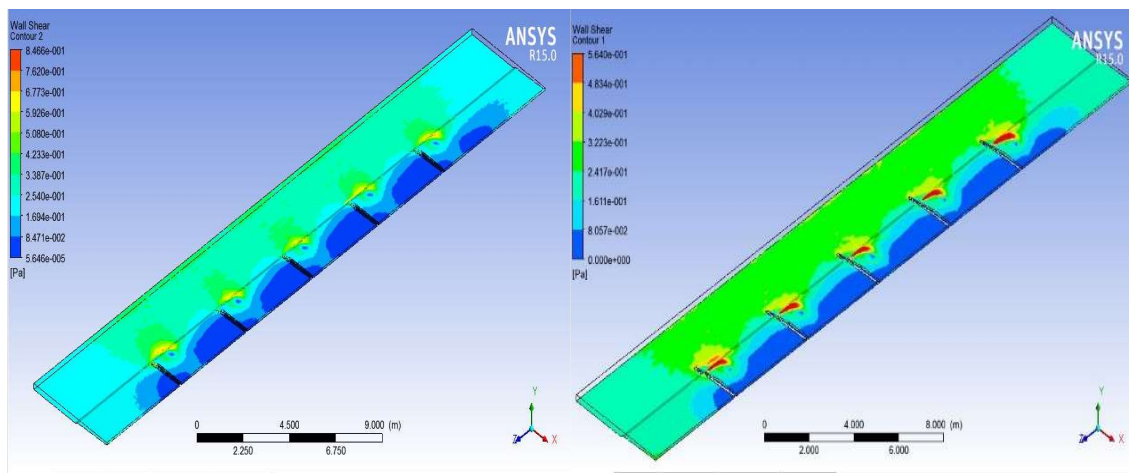
Figure 4.9 Shear Stress on bed for M1 & M2 Model
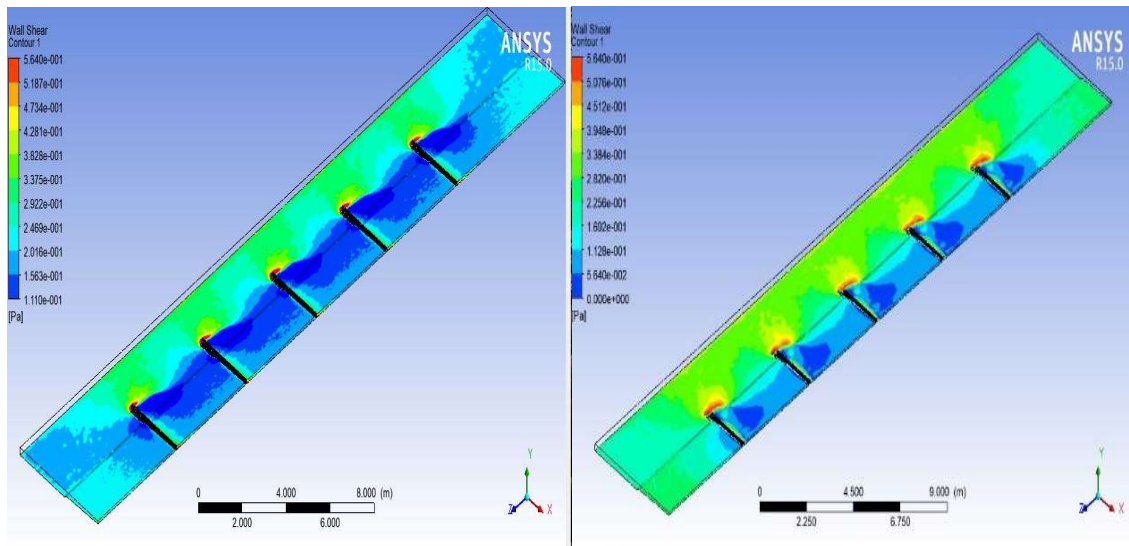
Figure 4.10 Shear Stress on bed for M3 & M4 Model
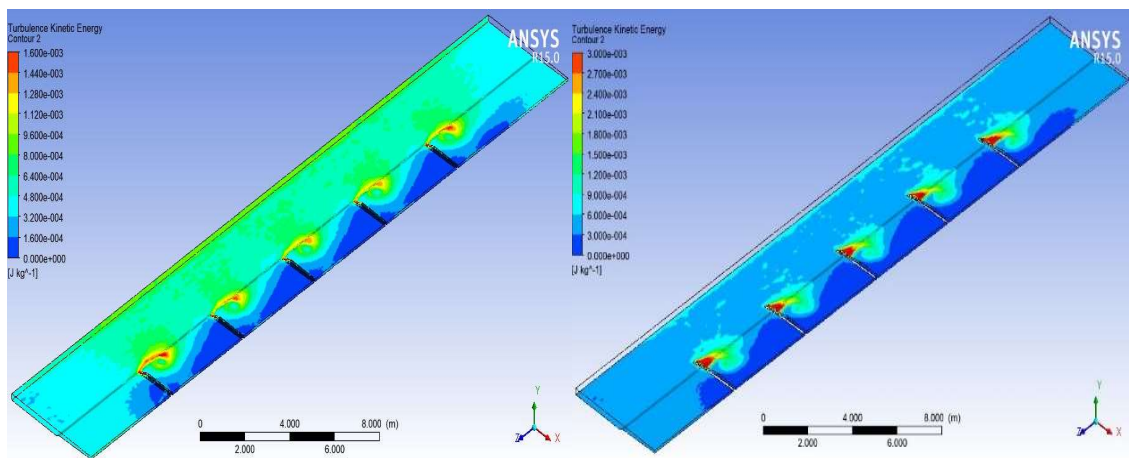
Figure 4.11 TKE contour for M1 & M2 model
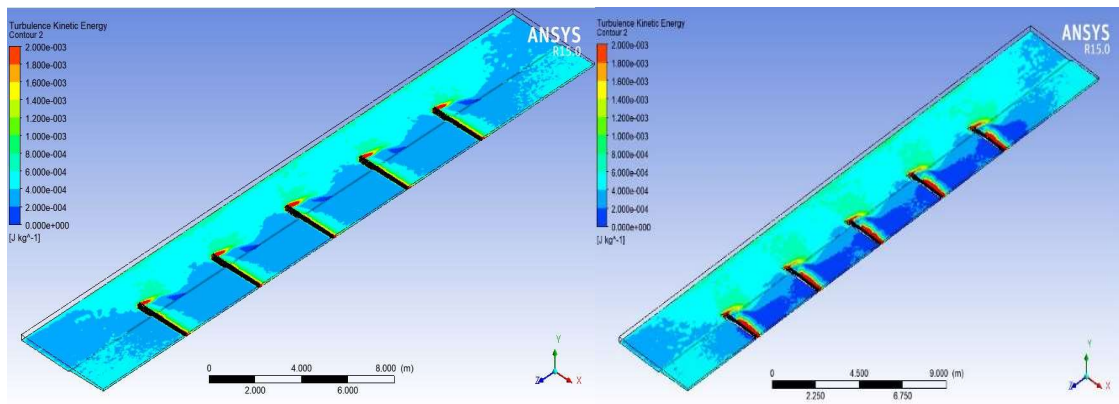
Figure 4.12 TKE contour for M3 & M4 model

Chapter 5 RESULTS AND DISCUSSION

5.1 Results Based on Tip Velocity

As the flow become stable after 3rd or 4th groyne so we have taken 4th groyne tip velocity for the study of tip velocity variation.

In the numerical analysis it is found that if we took the tip of 1st groyne in the series of five groynes then the magnitude of velocity always gets amplified up to 2 times but near the tip of 4th groyne, flow already gets shifted towards centre of channel so tip velocity always remains less than that of free flow velocity. The tip velocity found to follow similar pattern that was drawn with the help of experimental results, with the slight variation which can be said to be in permissible limit, just downstream of the tip there is increase in the velocity of flow.
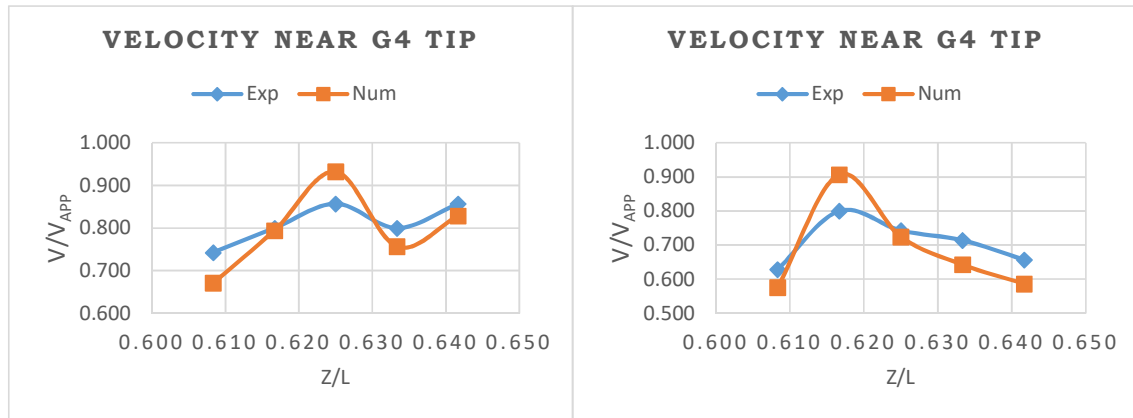
Figure 5.1 tip velocity for M1 & M2 model
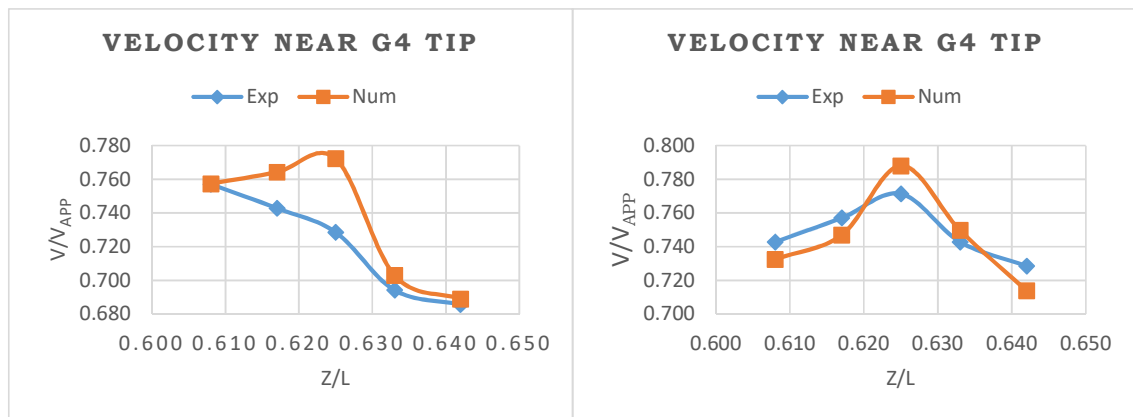
Figure 5.2 tip velocity for M3 & M4 model

Normally velocity near the tip remains close to 0.75 times the flow velocity but it is increased up to 0.95 times the flow velocity. As permeability of the groyne is increased the variation of velocity in vicinity of tip get reduced also the amplification factor gets reduced. M1 model completely obstruct the flow so creating more disturbance as compare to M2 model in which due to inclination of tip obstruction pattern changes.

5.2 Results Based on Velocity Variation at Location Relative to Protected Bank

For studying the effect of different layout of the groynes different locations are chosen relative to the protected bank. Here X/B ratio shows the distance of location on which graph is drawn away from the protected bank.

Graph in fig 5.3 shows the velocity variation on the furthest location to protected bank, as the length of intrusion of M3 groyne is largest so the velocity amplification is greatest. The effect of other models are quite small due to their smaller length.
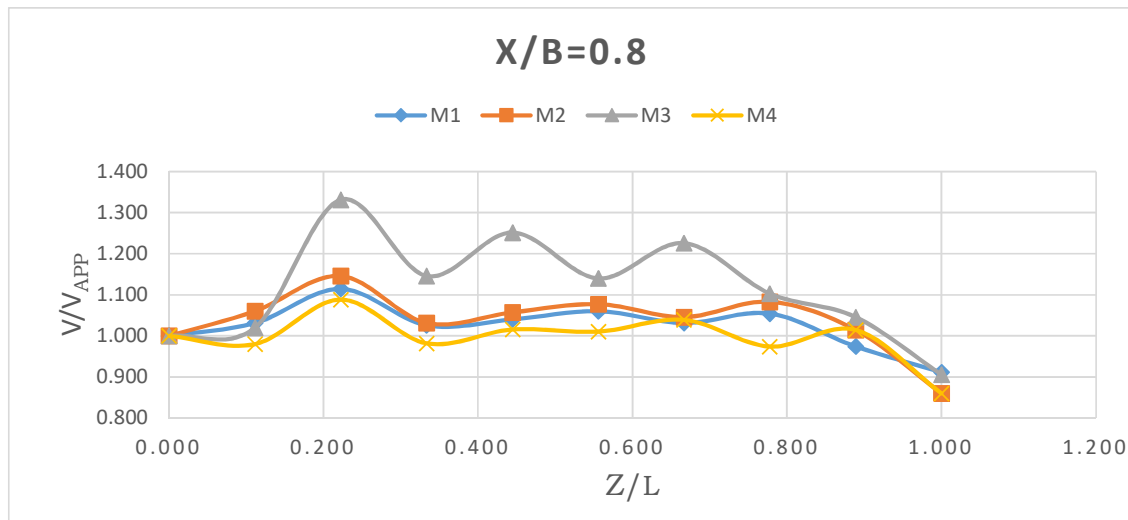
Figure 5.3 velocity variation for X/B=0.8

As we move closer to centre of the channel the amplification of velocity due to M2 and M4 model gets increased and due to M3 model get reduced due to permeability in M3 model groynes, this can be seen in graphs shown in fig 5.4. In comparison of M4 model, the amplification factor is more in case of M2 model due to completely impervious layout of the M2 model groynes. Once we

move in location in which length of intrusion is more than distance of location from protected bank, then in M3 model the velocity amplification factor gets reduced to less than 1 and it almost keep constant due to the permeability of groynes (in M3 model) over its whole length. This is shown in graph drawn in fig 5.5.
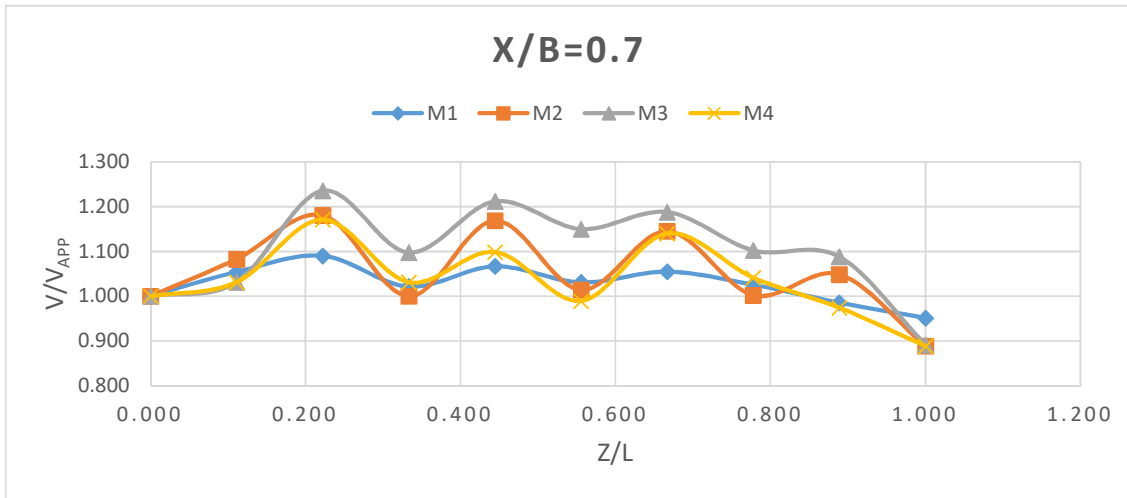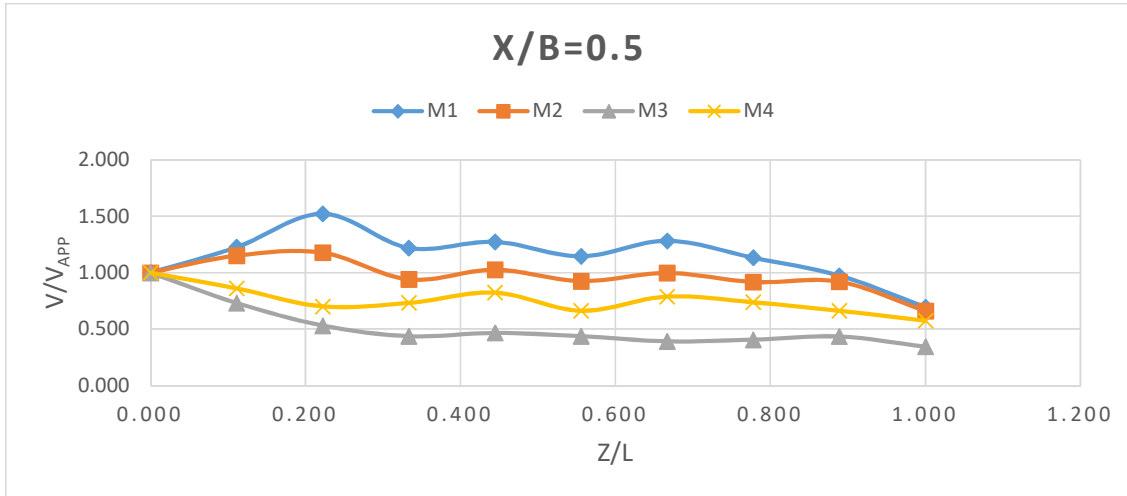

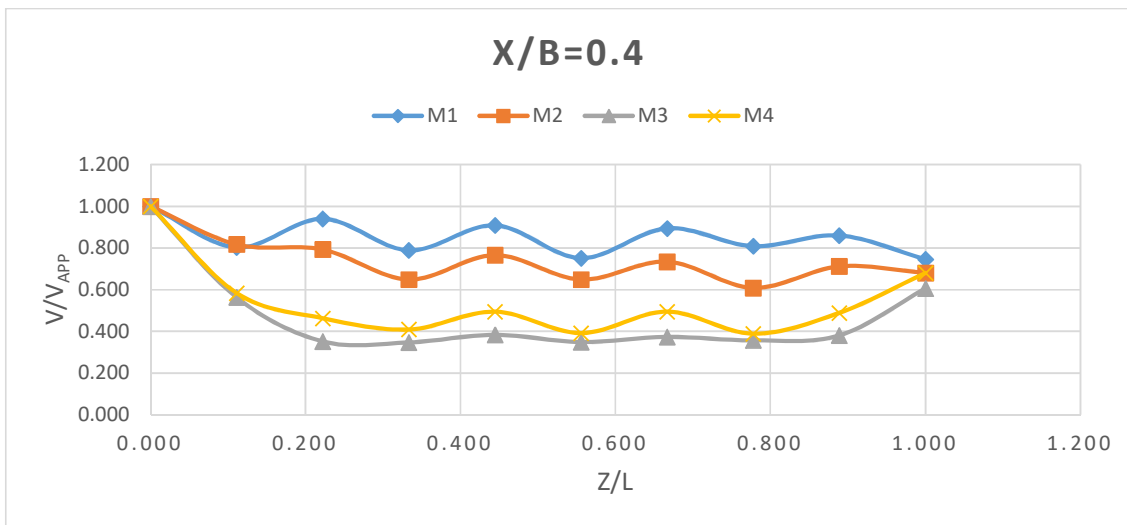**Figure 5.4 velocity variation for X/B=0.7**
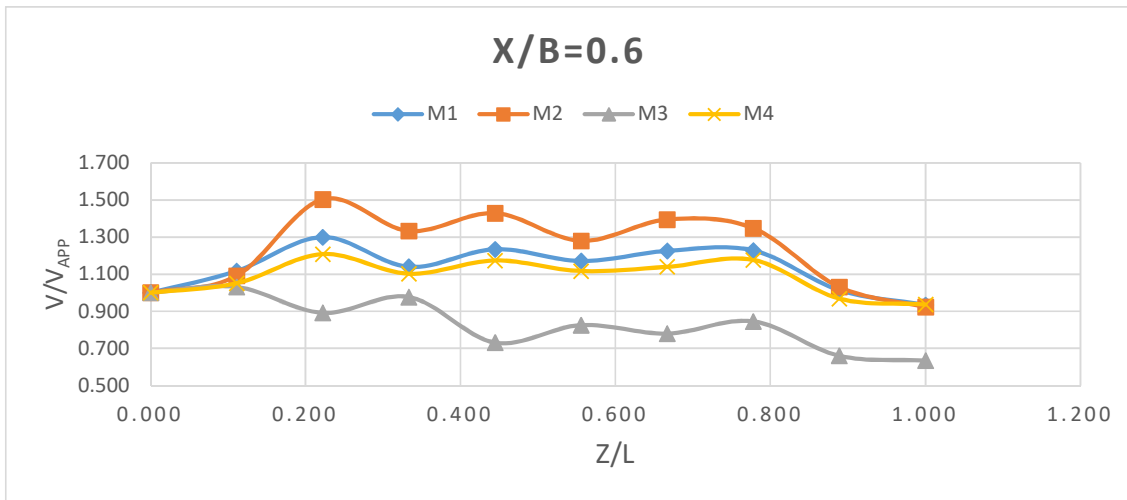
Figure 5.5 Velocity Variation for X/B=0.6

For location at the centre of the channel the amplification factor for M3 and M4 model reaches to the value which is less than 1 and for M2 model it is close to 1 as this region for M2 model groynes is mixing zone for mainstream and flow in groyne field. But for M1 model amplification factor became close to 1.4 as the length of groyne is less than half width of channel. This can be seen in graph shown in fig 5.6.

Figure 5.6 Velocity Variation for X/B=0.5

For X/B=0.4 location, velocity is more for M1 and M2 model as compare to others. For permeable groyne, the variation of velocity in this location remains almost constant.

**Figure 5.7 Velocity Variation for X/B=0.4**

At the location which falls inside the intrusion length of all type of model groynes, the velocity amplification ratio in M3 and M4 model is more as compare to others due to their permeability whereas for M1 and M2 model a kind of stagnation zone is formed due to which amplification factor is low. This can be seen in graph drawn in fig 5.8.
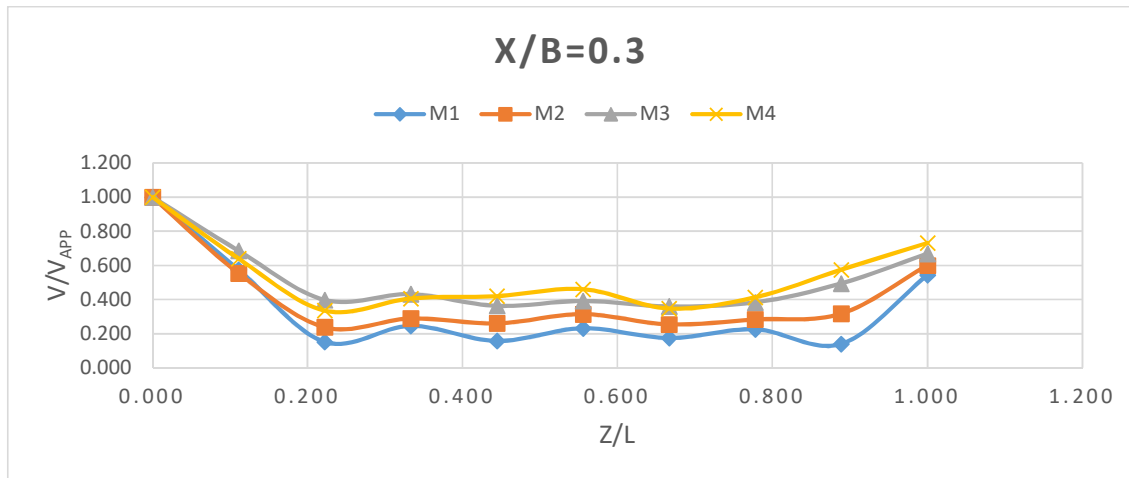
Figure 5.8 Velocity Variation for X/B=0.3

5.3 Results Based On Shear Variation at Location Relative to Protected Bank

For the study of shear stress variation on bed of channel over the flow field similar approach is taken as for the study of velocity variation. Results shown by the shear variation on different location relative to the protected bank is similar to that of velocity variation but with different values of amplification value.
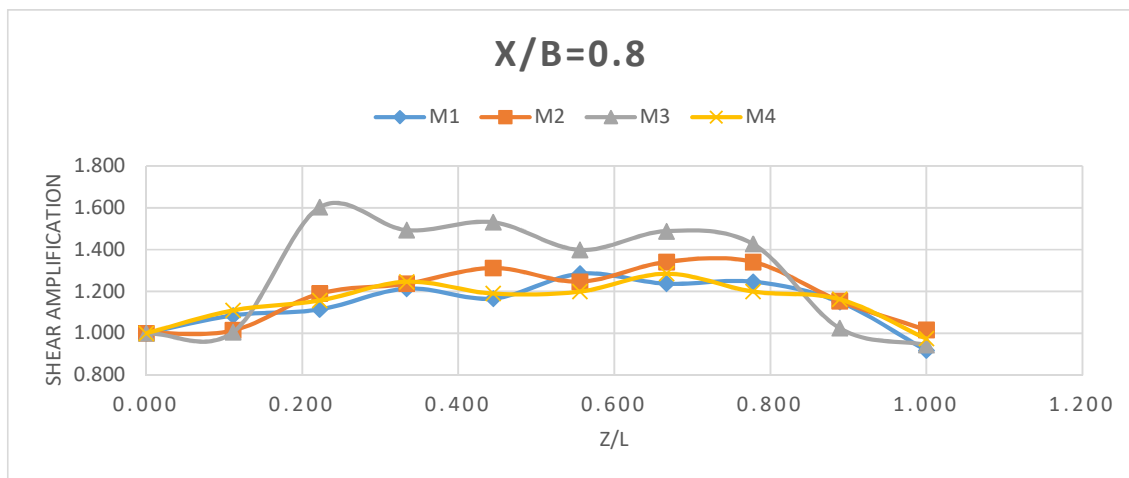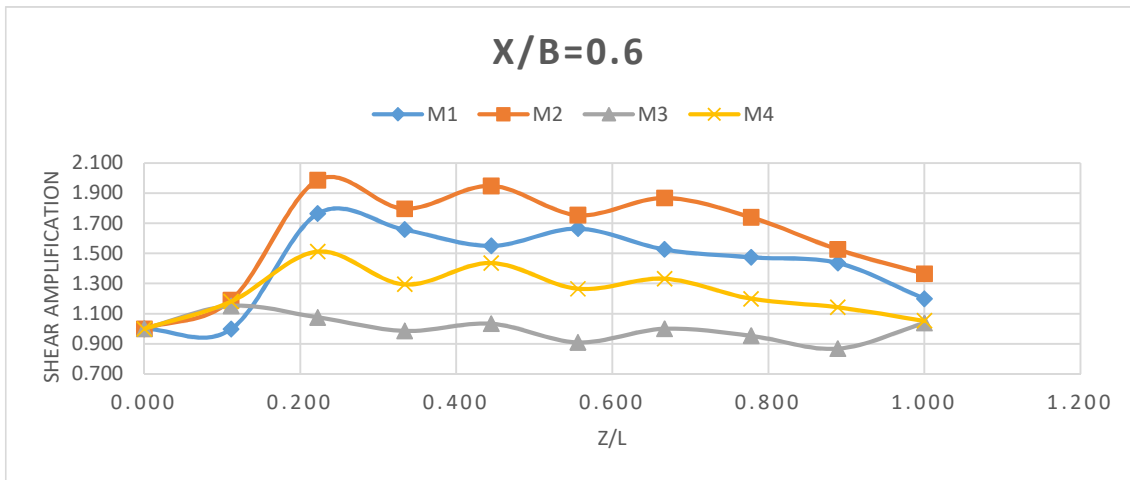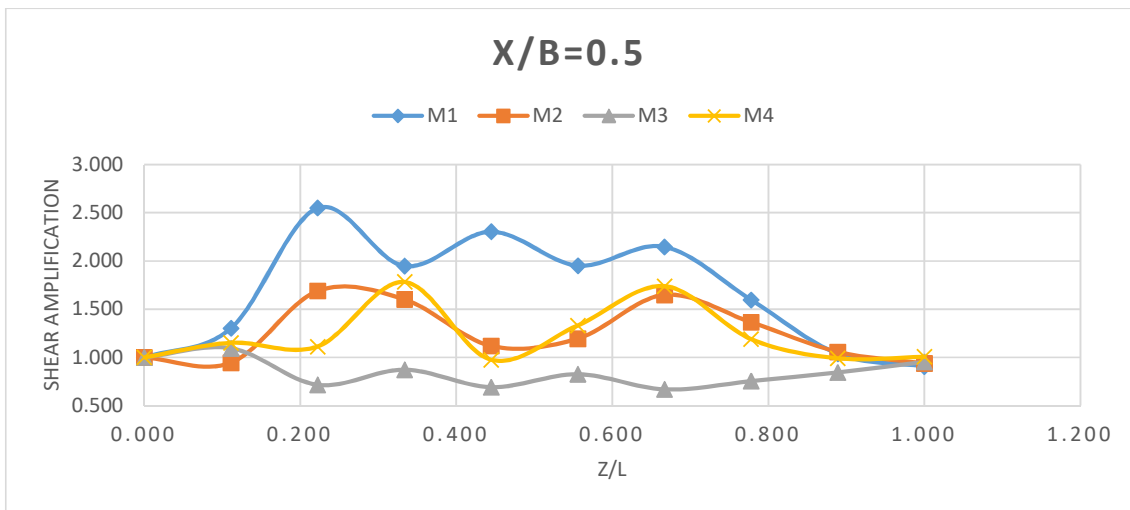

Figure 5.9 Shear Variation for X/B=0.8

As we move towards the centre of channel from opposite bank the shear values for M3 models starts decreasing whereas for M1 and M2 model shear values start increasing, this is due to the fact that intrusion length is more for M3 as compare to others.
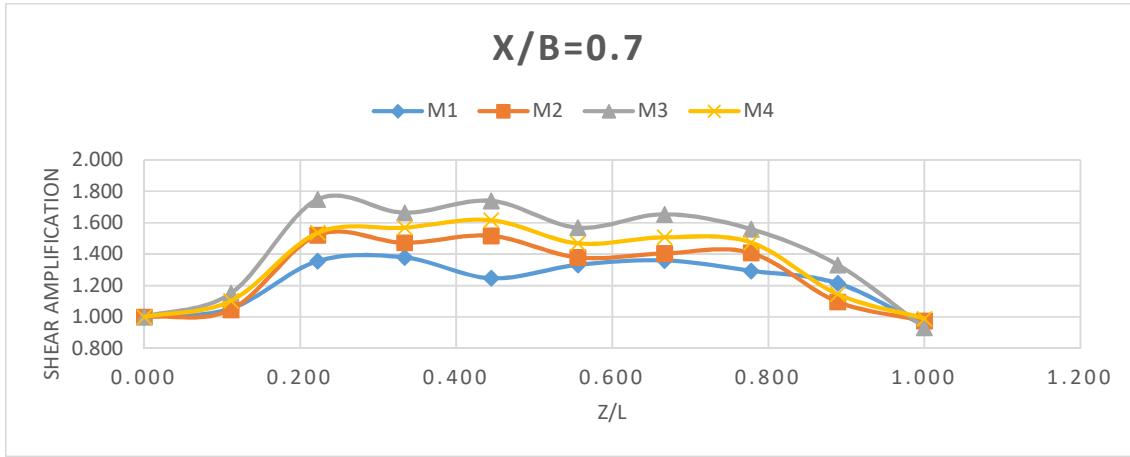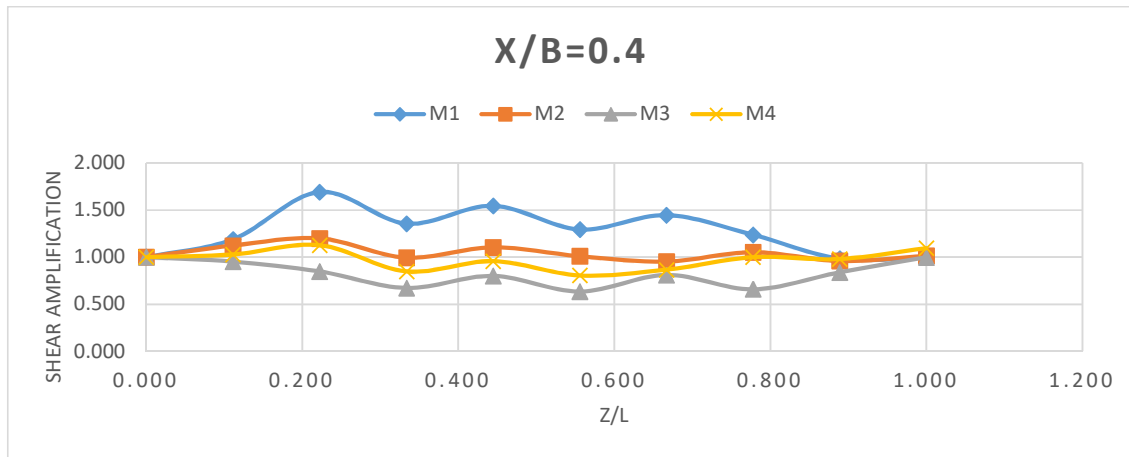
Figure 5.10 Shear Variation for X/B=0.7

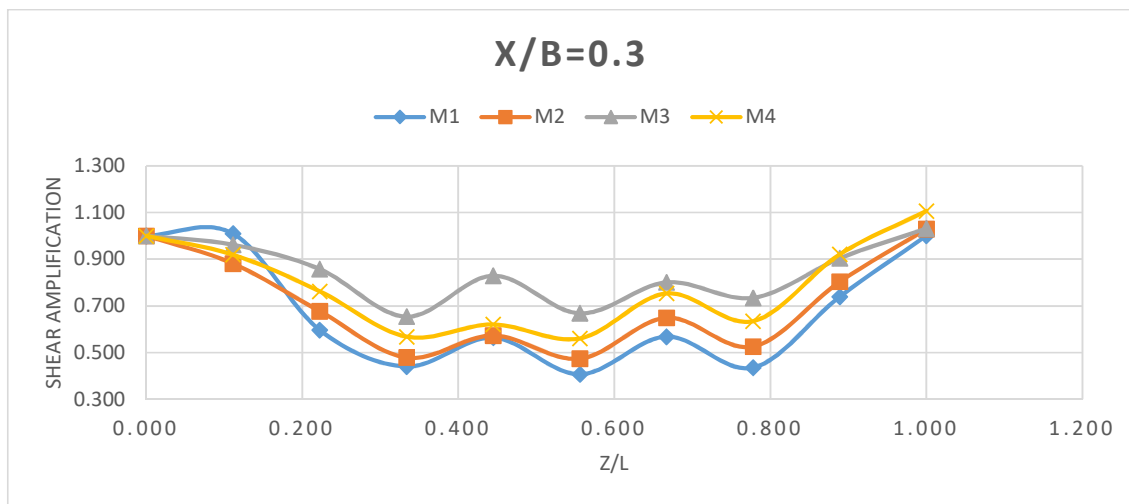**Figure 5.11 Shear Variation for X/B=0.6**

Figure 5.12 Shear Variation for X/B=0.5

Figure 5.13 Shear Variation for X/B=0.4

In region close to protected bank the shear stress gets reduced to small value for M1 and M2 model due to stagnation of flow in this region. For M3 and M4 model due to their permeability value of shear stress remain similar to other section lies within their respective intrusion length.

Figure 5.14 Shear Variation for X/B=0.3

5.4 Results Based On Vertical Velocity Profile

At the critical location, velocity are plotted on vertical plane to calculate the gradients, which can be directly related to the shear stress. As graph on fig 5.15 shows that the velocity gradient is more in case of M1 and M2 groyne as compare to M3 and M4 groyne. This can be attributed to the inclusion of permeability in latter two models, due to permeability the velocity variation

over the depth is get reduced. In case of M4 model, the velocity gradient is similar to M3 model but velocities are more as compare to other model this could be due to the lower portion of the groyne in M4 is impermeable hence providing less area of flow over the tip, resulting in higher velocity.
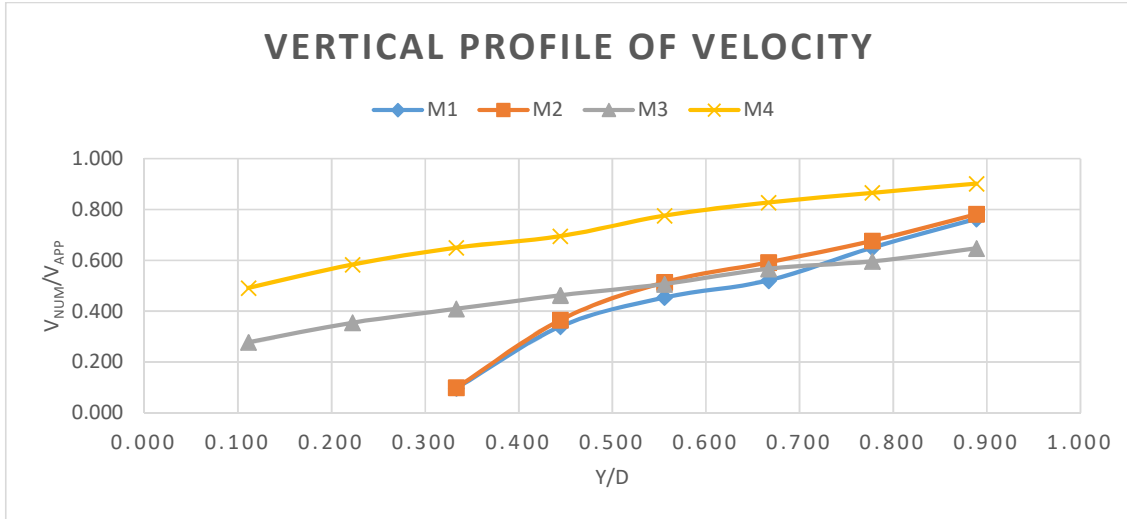

Figure 5.15 Vertical Profile of Velocity

5.5 Results Based On Horizontal Profile of Velocity

Variation of velocity in horizontal plane can be used to study the chances of vortex formation. As chances of flow becoming circular then chances of formation of scour hole increases.
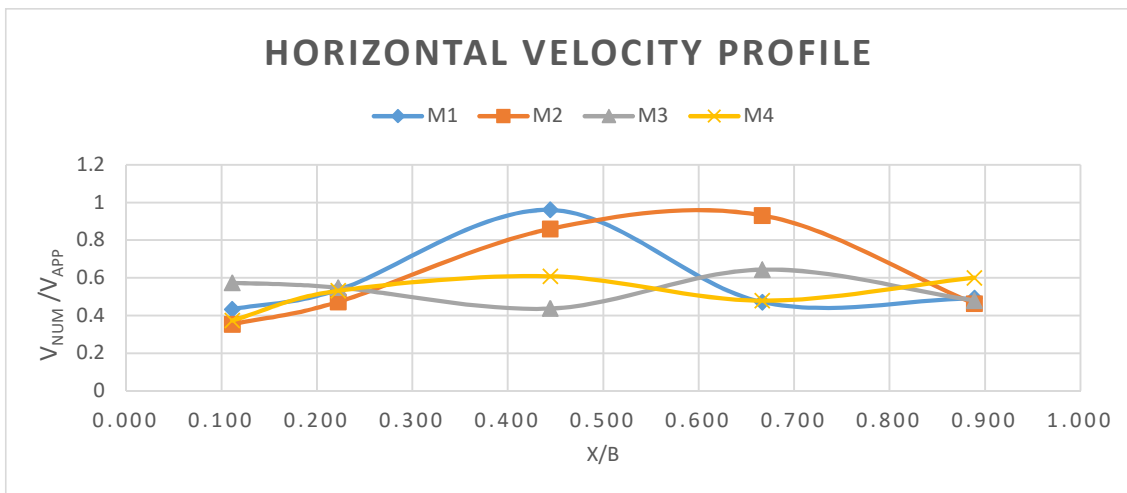

Figure 5.16 Horizontal Profile of Velocity

From graph shown in fig 5.16, it can be seen the variation of velocity over the centre region of width of channel is more in case of M1 and M2 model, due to this reason the chances of circular motion near the tip. Fig 4.1 & 4.2 shows the formation of vortex near the groynes. In case of M3 & M4 model, the variation in the velocity across the width is less so the streamline remains almost straight shown in fig 4.3 & 4.4.

5.6 Results Based On Variation of TKE

Variation of TKE at different location in respect of protected bank is shown in fig 5.17. Location close to protected bank the TKE value of M3 model is higher than the others due to the permeability of the groyne. The maximum values for different models can be found out near to the location of their tips. In region which close to opposite bank, the value of TKE is get reduced due to the reason that the effect of groynes is almost ended up.
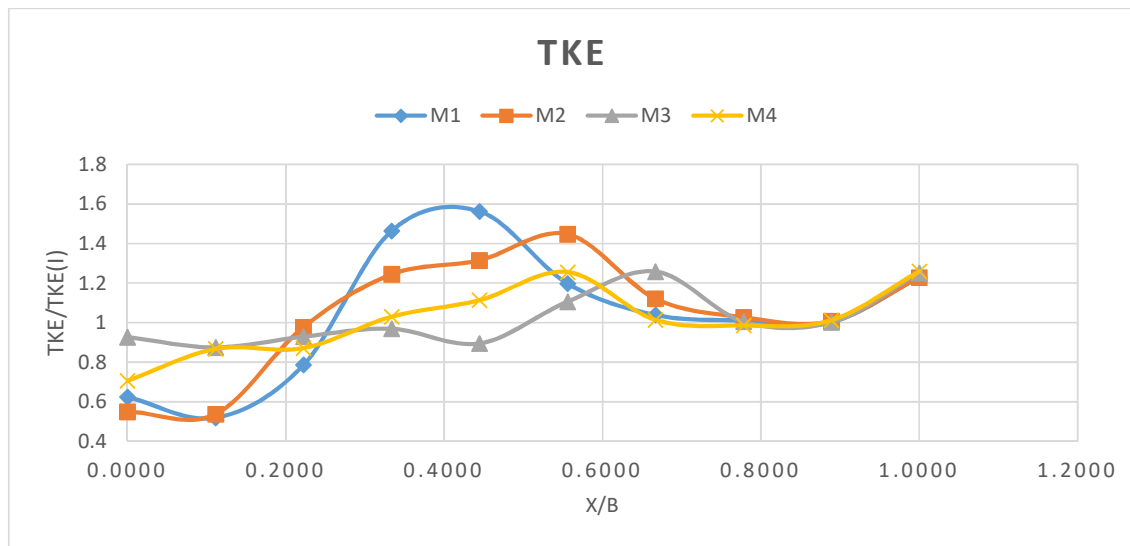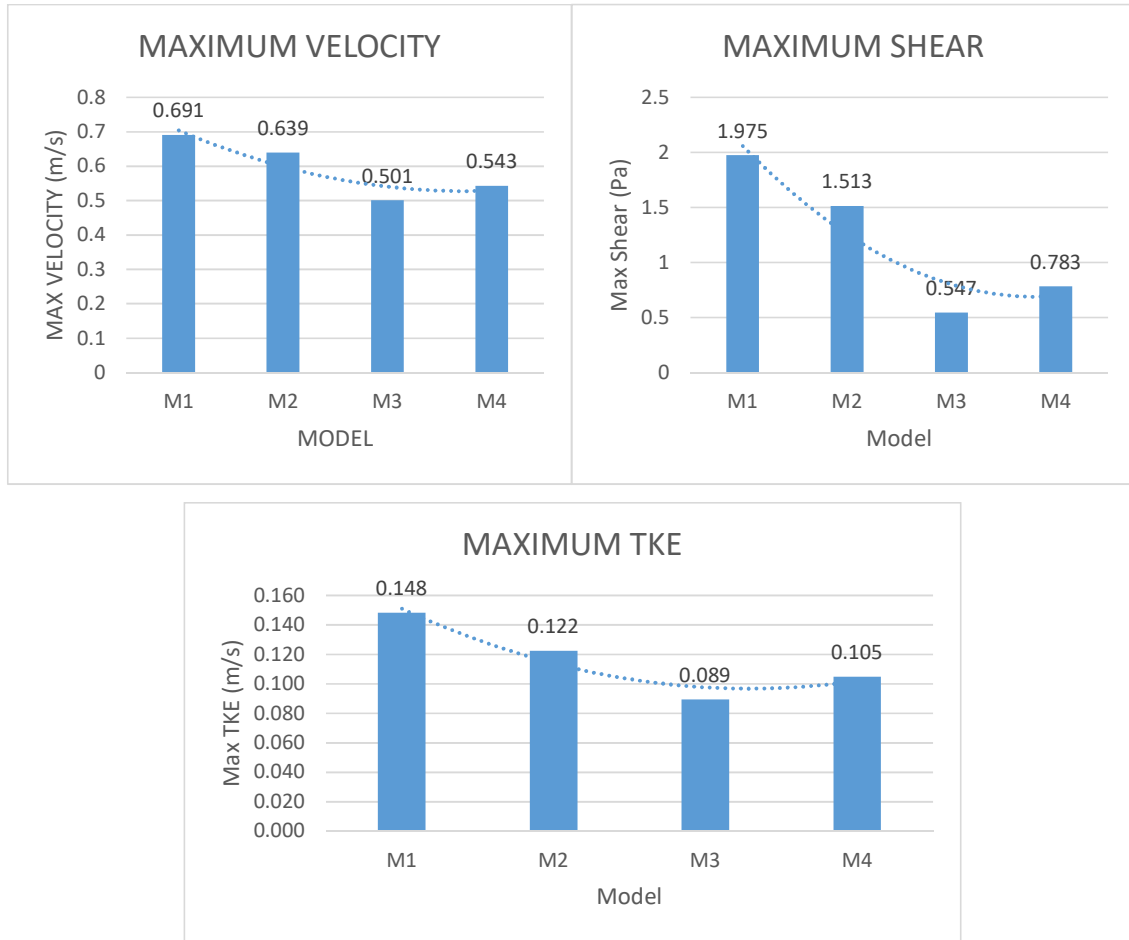

Figure 5.17 TKE Variation on Horizontal Place

5.7 Results Based On Maximum Values

The maximum value of velocity, shear, TKE for different models are shown in fig 5.18. Maximum velocity and its location can be of interest due to the region that it can give idea of location of scour hole which is an important consideration for groyne stability. Table 4.14 shows the values and location of maximum velocity, from the table we can see that for M1 and M2 model the

location of maximum velocity is away from the groyne in comparison to M3 and M4 model.

MAXIMUM VELOCITY

0.691
0.639
0.501
0.543

MAX VELOCITY (m/s)

0.8
0.7
0.6
0.5
0.4
0.3
0.2
0.1
0

M1   M2   M3   M4

MODEL

MAXIMUM SHEAR

1.975
1.513
0.547
0.783

Max Shear (Pa)

2.5
2
1.5
1
0.5
0

M1   M2   M3   M4

Model

MAXIMUM TKE

0.148
0.122
0.089
0.105

Max TKE (m/s)

0.160
0.140
0.120
0.100
0.080
0.060
0.040
0.020
0.000

M1   M2   M3   M4

Model

Figure 5.18 Plots of Maximum Values

Similarly, values of maximum shear stress, TKE and their location is important as they can give us idea of location where there are more chances of scouring or formation of eddies. Location of maximum shear and TKE show similar pattern shown by velocity.

Chapter 6 CONCLUSION

6.1 Conclusion Based On Tip Velocity

1. Study of tip velocity is done around the fourth groyne is done to show that the results found by numerical modelling is in resonance with the experimental results.

6.2 Conclusion Based On Velocity Variation

2. After seeing velocity variation for single model it can be concluded that the variation near to first two groynes are more and after 3rd groyne flow gets stabilise. So from this, it could be understood that the behaviour of first two groyne is different from the groynes placed downstream to them.

3. From velocity variation on different location relative to protected bank, we can conclude that in case of M1 and M2 model there is formation of stagnation zone near the protected bank where flow velocity is quite small.

4. M3 and M4 model provide uniform variation of velocity within their intrusion length, but as intrusion length is more for M3 model the velocity near the opposite bank is more in comparison to other model.

5. Point of maximum velocity for impermeable groyne is away from the groyne tip but for permeable groyne, it is closer to tip of groyne.

6.3 Conclusion Based On Variation of Shear Stress over the Bed

6. Shear stress on protected bank of M1 and M2 model is quite small as the disturbance is low but near the tip it has quite high value, increasing the chances of scour

7. For M3 and M4 model it is uniformly distributed over the length and near the tip, it value increases with smaller amplification factor.

6.4 Conclusion Based On TKE Variation

8. TKE for impermeable groyne is more as compare to permeable groyne. So for M1 and M2 model, TKE is more as compare to other model.

6.5 Overall Conclusion

9. The main objective of the study is to obtain better layout of groyne out of 4 used. From various numerical data obtained, it can be said that in most of the parameter performance of M3 model is better but the location of maximum shear and TKE for M3 model is close to opposite bank.

10. This problem of M3 model is due to fact that it has more intrusion length which can be overcome by using M4 model which is combination of both impermeable and permeable groyne.

11. For same area block the intrusion length of M1 model is less but parameters like shear, velocity, TKE is get amplified near the tip. For M3 model the intrusion length is more which causes shifting of critical location towards opposite bank. Advantages of both M1 and M3 model is included in M4 model, so it can be labelled as better option than other models analysed.

6.6 Future Scope of Study

In this study, the groynes are under emerged condition so in future numerical modelling can be done for submerged condition. Study related to sediment transport in the flow field can also be included for better understanding the flow patterns. Studies related to the spacing between the groynes and separation length for different groynes can also be done for improving the performance of groyne models.

REFERENCES

[1] Acharya, Anu, Duan, J, G. "Three-Dimensional Simulation Of Flow Field Around Series Of Spur Dikes", ASCE copyright Proceedings of the 2011 World Environmental and Water Resources Congress, California, USA. 2011.

[2] Ahmed, H. S., Hasan, M. M., Tanaka, N. "Analysis Of Flow Around Impermeable Groynes On One Side Of Symmetrical Compound Channel: An Experimental Study", Journal of Water Science and Engineering (2010).

[3] Asayama, Chiharu. "Study on Control for Suitable Bed Morphology around Successive Groynes".

[4] Baba, Y., et al. "Flows and Bed Load Dynamics around Spur Dyke in a Compound Channel" 11th International Symposium on River Sedimentation (ISRS), 2010.

[5] Burele, S., Gupta, I.D., Sharma, N. "Experimental Study on Performance of Spurs", ISH Journal of Hydraulic Engineering, September 2012.

[6] Duan, Jennifer, G. "Mean Flow and Turbulence around a Laboratory Spur Dike" Journal of Hydraulic Engineering, 2009.

[7] Ettema, R. and Muste, M. "Scale Effects in Flume Experiment on Flow around a Spur Dike in Flatbed Channel", Journal of Hydraulic Engineering, July 2004.

[8] Ghaldarbandi. R., Keshavarz, M. H., Hakimzadeh, H. "Investigation of the Bed and Structural Slopes on Bed Shear Stress and Flow Characteristics around an Impermeable Groyne", Journal of Hydraulic Structures, 2013.

[9] Kafle, Mukesh, R. "Numerical Simulation of Flow around a Spur Dike with Free Surface Flow in Fixed Flat Bed." Journal of the Institute of Engineering, 2014.

[10] Kang, Joongu, "Experimental Investigation on the Local Scour Characteristics around Groynes Using a Hydraulic Model." Water and Environment Journal, 2011.

[11] McCoy, A., Constantinescu, G. "Numerical Investigation of Flow Hydrodynamics in a Channel with a Series of Groynes".

[12] Minor, B., Jamieson, E., Rennie, C. D., Townsend, R. D. "Three-Dimensional Flow in A Barb Field" Department of Civil Engineering, University of Ottawa, Canada.

[13] Ouillion, S., Dartus, D. "Three-Dimensional Computation of Flow around Groyne", Journal of Hydraulic Engineering, Vol. 123, Issue 11, November 1997.

[14] Rajaratnam, N., Nwachukwu, B. A. "Flow near Groin-Like Structures", Journal of Hydraulic Engineering, Vol. 109, Issue 3, January 1983.

[15] Safarzadeh, A., et al. "Experimental Study of Head Shape Effects On Shear Stress Distribution around a Single Groyne", Proceedings of 5th International Conference on Fluvial Hydraulics, 2010.

[16] Schmidt, J. C. "Flume Simulation of Recirculating Flow and Sedimentation", Water Resource Research (1993).

[17] Shahrokhi, Mahdi, Sarveram, H. "Three-Dimensional Simulation of Flow around A Groyne with Large-Eddy Turbulence Model", Journal of Food, Agriculture & Environment 9.3&4, 2011.

[18] Sukhodolov, A., Engelhardt, C., Krüger A., Bungartz, H. "Case Study: Turbulent Flow and Sediment Distributions in a Groyne Field", Journal of Hydraulic Engineering, Vol. 130, Issue 1, January 2004.

[19] Tambe, R.K., Kulkarni, D., Talegaonkar, S.D. "Studies of Spacing of Permeable Spurs in Series", IJCIET, volume 8. Issue 5, May 2017.

[20] Tingsanchali, T., Maheswaran, S. "2-D Depth-Averaged Flow Computation near Groyne", Journal of Hydraulic Engineering, Vol 116, Issue 1, January 1990.

[21] Uijttewaal, W.S.J. "Effects of Groyne Layout on the Flow in Groyne Fields: Laboratory Experiments", Journal of Hydraulic Engineering (2005).

[22] Uijttewaal, W. S. J., Lehmann, D., Mazijk, A. "Exchange Processes between a River and Its Groyne Fields: Model Experiments", Journal of Hydraulic Engineering, Vol 127, Issue 11, November 2001.

[23] Weitbrecht, V., Jirka, G.H. "Flow Patterns and Exchange Processes in Dead Zones of Rivers" (2001).

[24] Yazdi, J., Sarkardeh, H., Azamathulla, H. Md., Ghani, A. "3D Simulation of Flow Around A Single Spur Dike With Free-Surface Flow", International Journal of River Basin Management (2010).

[25] Yeo, H. K., Kang, J. G., Kim, S. J. "An Experimental Study on Tip Velocity and Downstream Recirculation Zone of Single Groynes of Permeability Change", KSCE Journal of Civil Engineering, Volume 9, January 2005.

[26] Yossef, M. F. M., Vriend, H. J. "Flow Details near River Groynes: Experimental Investigation" American Society of Civil Engineers (2011).

[27] Zhang, Hao, et al. "Experiment Study on Channel Bed Characteristics around Spur Dykes of Different Shapes." Journal of Japan Society of Civil Engineers, 2013.